ECMWF COPERNICUS REPORT

Copernicus Atmosphere Monitoring Service

User Guide to the CAMS Radiation Service (CRS)

Status December 2025

Issued by: DLR / M. Schroedter-Homscheidt

Date: 15/02/2026

Ref: CAMS2_73_bis_2025SC1_D73.3.2.1_2025_UserGuide_v1

User Guide to the CAMS Radiation Service

Status December 2025

DLR
Marion Schroedter-Homscheidt
Jorge Lezaca

ARMINES
Mireille Lefèvre
Yves-Marie Saint-Drenan

VAISALA FRANCE
Laurent Saboret
Prashanth Victor

For citations in peer-reviewed journals on the CAMS Radiation Service methods please use:

- Schroedter-Homscheidt et al., Surface solar irradiation retrieval from MSG/SEVIRI based on APOLLO Next Generation and HELIOSAT-4 methods, Meteorol. Z./Contrib. Atm. Sci., doi: 10.1127/metz/2022/1131
- Qu, Z. et al., 2017. Fast radiative transfer parameterisation for assessing the surface solar irradiance: The Heliosat-4 method, Meteorol. Z., 26, 33-57, doi: 10.1127/metz/2016/0781.
- Gschwind, B., et al., 2019. Improving the McClear model estimating the downwelling solar radiation at ground level in cloud free conditions – McClear-V3., Meteorol. Z., doi:10.1127/metz/2019/0946.
- Lefèvre, M. et al, 2013. McClear: a new model estimating downwelling solar radiation at ground level in clear-sky conditions. AMT, 6, 2403-2418, doi: 10.5194/amt-6-2403-2013.

Table of Contents

1. Introduction 7

1.1 Acronyms and definitions 9

2. The CAMS Radiation Service in a nutshell 11

2.1. The CAMS All-Sky Radiation Service in a nutshell 11
2.2. The CAMS Clear Sky Radiation Service in a nutshell 12
2.3. How to cite CAMS Radiation Service data 13

3. The legacy methods 14

3.1. History of the Heliosat methods 14
3.2. Overview of the Heliosat-2 method 16
3.3. Inputs to clear-sky models 18
3.3.1. Aerosols 18
3.3.2. Water vapour 18
3.3.3. Ozone 18
3.3.4. Linke Turbidity 18
3.3.5. Known problems with input data in the legacy databases 19

4. The Heliosat-4 method 20

4.1. Concept of Heliosat-4 20
4.2. Schematic view of the Heliosat-4 method 22
4.3. Overview of the McClear model 22
4.4. Overview of the McCloud model 24
4.5. Computation of the SSI 27
4.6. Practical implementation 28
4.7. Bias correction 29

5. Known problems in the retrieval of the SSI 30

5.1. Sub-pixel phenomena 30
5.2. Change in terrain elevation within a grid cell in databases 30
5.3. Coastal sites 32
5.4. Satellite viewing angles larger than 60° 32
5.5. Bidirectional reflectance and albedo 32
5.6. Cloud vertical position and parallax effects 33
5.7. Systematic biases if comparing against BSRN ground observations 33

6. The CAMS Radiation Service 34

6.1. The operational chain 34
6.2. Description of the CAMS Radiation Service Information System 35
6.2.1. The CAMS Radiation Service Information System as a GEOSS component 35

6.2.2. Web Processing Service (WPS) 37

7. The CAMS Radiation Data 38

7.1. Data policy/Licence 38
7.2. Parameters 38
7.3. CRS - time series datasets 40
7.3.1 Detailed info expert output mode 40
7.3.2 How to make a request for a CAMS Radiation Service time series 42
7.3.3 Format of products 43
7.3.3.1 Data formats 43
7.3.3.2 Metadata 43
7.4. CRS - gridded dataset 44

8. Validation 46

8.1. Principles and limitations 46
8.2. Overview of the validation activities 47

9. References 50

Executive Summary

The European Earth observation programme Copernicus aims at providing environmental information to support policymakers, public authorities and both public and commercial users. A systematic monitoring and forecasting of the state of the Earth's subsystems is provided within six thematic areas: marine, land, atmosphere, emergency, security, and climate change.

The pre-operational atmosphere service was provided through the FP7 projects MACC and MACC-II/-III (Monitoring Atmospheric Composition and Climate). Since 2016 this is continued in the operational Copernicus Atmosphere Monitoring Service (CAMS). CAMS combines state-of-the-art atmospheric modelling with Earth observation data to provide information services covering European Air Quality, Global Atmospheric Composition, Climate, and UV and Solar Energy. Within the CAMS Radiation Service (CRS) existing historical and daily updated databases for monitoring incoming surface solar irradiance are made available. The service meets the needs of European and national policy development and the requirements of (commercial) downstream services (e.g. planning, monitoring, efficiency improvements, and integration into energy supply grids).

CAMS Radiation Service is subject to continuous validation and development. The User Guide describes the data, methods and operations used to deliver time-series as primary product. It also describes how a gridded dataset as a combination of time series on a regular latitude/longitude grid is generated in a post-processing.

Section 2 includes a short description of the **CAMS Radiation Service 'in a nutshell'**. It is meant for the 'fast-track readers' as a first orientation.
Section 3 describes shortly the previously provided databases HelioClim-3 and SOLEMI. The **historical evolution of Heliosat methods** used to convert satellite images into solar surface irradiance is shortly presented as users often reported the need for a version summary as the published literature is hardly accessible and the used wording partly heterogeneous.
Section 4 describes the **Heliosat-4 method**, including the **McClear** model describing the irradiance under clear-sky (cloud-free) conditions, and its different versions. Heliosat-4 is the method used to produce the irradiances in the CRS.
Section 5 summarizes **existing knowledge and lessons learnt** on satellite-based irradiances, which has been published previously only in a scattered manner and is hardly available to users.
Section 6 provides an overview of the **operations and the workflow**. It also discusses the means to control the quality in the processing chain.
Section 7 provides an overview on **available products**.
Section 8 introduces the method applied in the 3-monthly **validation reports**. It discusses the principles how validation results are presented and how they may be interpreted**. Quantitative validation results** can be found only in the 3-monthly validation reports itself. This includes results for a recent 3 month period in each report. In the 3rd report of each calendar year an overview aggregated for the last years is provided.

1. Introduction

The Atmosphere Monitoring Service of Copernicus (CAMS) combines state-of-the-art atmospheric modelling on aerosols with Earth observation data to provide information services covering European air quality, global atmospheric composition, climate, and UV and solar energy.

The CAMS Radiation Service provides a fast parameterisation of the radiative transfer in the atmosphere (Fig. 2-1) and couples cloud-free sky parameters as aerosols, water vapour, and ozone with satellite-based cloud information (Fig. 2-2).

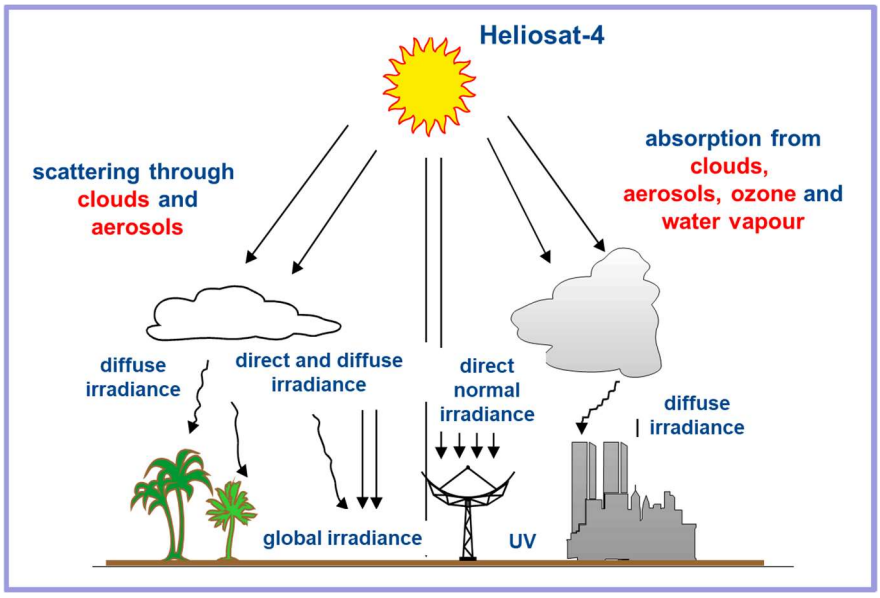

Fig. 2-1: Principle of radiative transfer which is the basis of the CAMS Radiation Service

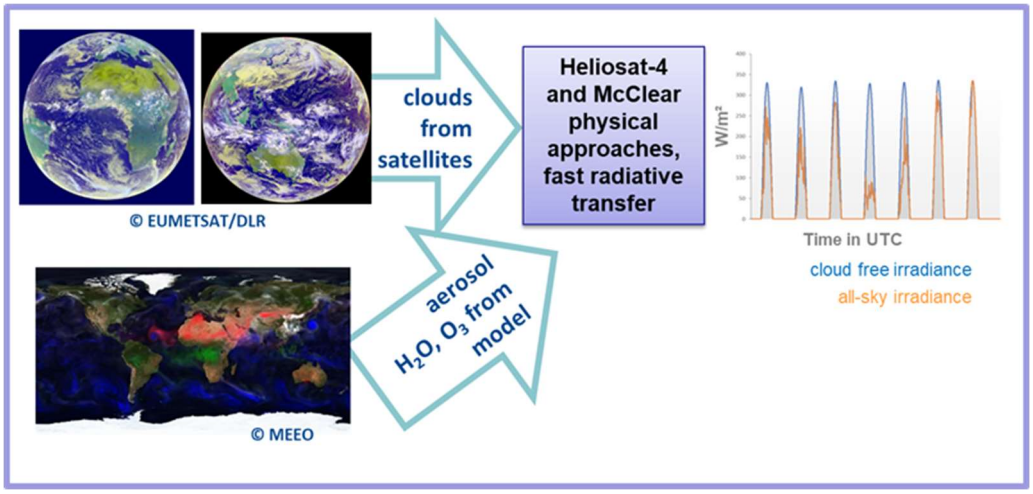

Fig. 2-2: Combination of satellite-based cloud information with model based aerosol, water vapour and ozone information to derive time series of solar radiation at the surface in cloudy and cloud-free conditions

The CAMS Radiation Service collects several data originating from various sources. Many of them describe the optical state of the atmosphere, e.g., aerosol, water vapour and ozone contents over the atmospheric column. Others depict the ground properties, e.g., ground albedo and ground elevation. These are inputs to a model that simulates the scattering and absorption phenomena occurring in the atmosphere and affecting the solar radiation in its way downwards to the ground. The output of this model is solar radiation available at ground level that can be used to produce solar energy, either as heat or electricity. Data can be accessed by the Atmosphere Data Store (ADS, https://ads.atmosphere.copernicus.eu/datasets/cams-solar-radiation-timeseries) or via the SoDa portal (http://www.soda-pro.com/web-services/radiation/cams-radiation-service).

Users mainly require **long-term time series** at user-defined locations for system planning which is a on-the-fly processed primary product using always the most recent software version and input data as available at the time the request is made. The time series processing chain is updated continuously with recent input data.

Some system analysis studies may require also **gridded and pre-calculated data** over large geographical areas. A gridded product is provided over land and coastal surfaces in a pre-selected 15 min and 0.1° temporal and spatial resolution and updated on an annual basis.

Within the radiation service, existing historical and daily updated databases HelioClim-3 and SOLEMI for monitoring incoming surface solar irradiation were further developed. The CRS is jointly provided by DLR, Armines, and Vaisala France. The Monitoring Atmospheric Composition and Climate (MACC) project series prepared for the service provision, which is now operational as part of the Copernicus programme.

1.1 Acronyms and definitions

ADS	Atmosphere Data Store
AOD	Aerosol optical depth
APOLLO	AVHRR Processing scheme Over cLouds, Land and Ocean
APOLLO_NG	APOLLO Next Generation
ASCII	American Standard Code for Information Interchange
BHI	All-sky direct (beam) irradiation, i.e., the direct part of the surface solar downward irradiation integrated over 285 to 2800 nm available at ground level, on a horizontal surface. For cloudy atmospheres, both non-scattered and scattered radiation within the field-of-view of a pyrheliometer are taken into account.
BNI	All-sky Direct Normal Irradiation. Part of the radiation that is received from the direction of the sun by a plane facing the sun. For cloudy atmospheres, both non-scattered and scattered radiation within the field-of-view of a pyrheliometer are taken into account.
CAMS	Copernicus Atmosphere Monitoring Service
CRS	CAMS Radiation Service, a service being operational since 1st January 2016. A service delivering time-series of solar irradiation available at ground level, created by DLR, Armines, and Transvalor (nowadays Vaisala France) within the Copernicus Service. Time-series start on 2004-01-01 and end at current day-2 for the Meteosat and on 2016-01-01 for the Himawari satellites.
DHI	All-sky diffuse irradiation, i.e., the diffuse part of the surface solar downward irradiation integrated over 285 to 2800 nm available at ground level, on a horizontal surface. Part of the radiation that is received on a horizontal plane from all directions except that of the sun.
DLR	Deutsches Zentrum für Luft- und Raumfahrt e.V., German Aerospace Center
GHI	All-sky global irradiation, i.e., the surface solar downward irradiation integrated over 285 to 2800 nm available at ground level, on a horizontal surface
HelioClim-1	A service and a database containing daily solar irradiation available at ground level, created by Armines from Meteosat images in reduced spatial and temporal resolution. It covers the period 1985-2005.

HelioClim-3	A service and a database containing 15 min solar irradiation available at ground level, created by Armines from Meteosat images. It starts in February 2004 and is updated daily.
Heliosat	Name of a family of methods to convert images acquired by meteorological geostationary satellites into images of solar radiation available at ground level. For example, the databases HelioClim-1 and -3 are constructed with the method Heliosat-2.
Heliosat-4	The new method for computing solar radiation at ground level.
MACC / MACC-II / MACC-III	Monitoring Atmosphere Composition and Climate. Three EC-funded research projects to establish the Copernicus Atmosphere Service before CAMS became operational.
MACC-RAD Service	The service within the MACC precursor projects that delivered MACC-RAD and McClear products on solar radiation at ground level until the end of 2015. Service delivery was replaced and continued by the CAMS Radiation Service on 1st January 2016.
McClear	A service delivering time-series of solar irradiation that should be observed at ground level if the sky were clear, created by Armines within the MACC / /MACC-II / MACC-III projects. Time-series start on 2004-01-01 and end at current day-2. It is operated now within the CAMS Radiation Service as the cloud-free 'clear-sky' model.
NASA-SRTM	National Aeronautics and Space Administration, Shuttle Radar Topography Mission
SoDa Service	A Web portal offering a one-stop access to several services (databases, applications) relating to solar radiation.
SOLEMI	Solar Energy Mining. It corresponds to both method and service providing SSI. It is a precursor service of CAMS Radiation Service at DLR, which is not operational anymore.
SSI	Surface Solar Irradiance, also called surface downward solar irradiance, or surface downward shortwave irradiance. It can also denote irradiation, which is the irradiance multiplied by a duration. For example, hourly irradiation is equal to the hourly average of irradiance multiplied by 3600 s.

2. The CAMS Radiation Service in a nutshell

2.1. The CAMS All-Sky Radiation Service in a nutshell

- Period of record: Feb 2004–present for Meteosat and Jan 2016 for Himawari satellite field of view, data is provided with up to 1 day delay
- Temporal resolution: 1 min, 15 min, 1 h, day, month
- Spatial coverage: Europe/Africa/Middle East/Eastern part of South America/Atlantic Ocean in the Meteosat field of view; part of Asia and Australia in the Himawari field of view
- Spatial resolution: Interpolated to the point of interest
- Data elements and sources: Global, direct, diffuse, and direct at normal incidence irradiation; global, direct, diffuse and direct normal irradiation in cloud free conditions; detailed expert mode with all atmospheric input parameters used for clouds, aerosols, ozone, water vapour, and the surface reflective properties.
  For cloudy atmospheres, the direct components (also known as beam components) include both non-scattered and scattered radiation within the field-of-view of a pyrheliometer.
- Data quality control and assessment: Input quality control, regular quarterly benchmarking against ground stations, regular monitoring the consistency and detecting possible trends.
- Availability:
  Copernicus Atmosphere Data Store
  https://ads.atmosphere.copernicus.eu/datasets/cams-solar-radiation-timeseries for time series at user-defined locations of interest and including the expert mode with detailed access to inputs used
  https://ads.atmosphere.copernicus.eu/datasets/cams-gridded-solar-radiation for a pre-calculated gridded dataset in 15 min and 0.1° latitude/longitude grid
- Data policy: This dataset is released for use under the CC-BY licence.
- Documentation:
  Dataset information at https://ads.atmosphere.copernicus.eu/datasets/cams-solar-radiation-timeseries?tab=documentation
  User's Guide accessible via https://ads.atmosphere.copernicus.eu/datasets/cams-solar-radiation-timeseries?tab=documentation

  Quarterly validation reports at https://atmosphere.copernicus.eu/supplementary-services

2.2. The CAMS Clear Sky Radiation Service in a nutshell

The fast clear-sky model called McClear implements a fully physical modelling replacing empirical relations or simpler models used before. It exploits the recent results on aerosol properties and total column content in water vapour and ozone produced by the Copernicus service. It provides irradiation that would be observed in cloud-free conditions.

- Period of record: 2004–present, data is provided with up to 1 day delay
- Temporal resolution: 1 min, 15 min, 1 h, day, month
- Spatial coverage: Global
- Spatial resolution: Interpolated to the point of interest
- Data elements and sources: clear sky (i.e. cloud free) global, direct, diffuse and direct at normal incidence irradiation; detailed expert mode with all atmospheric input parameters used for clouds, aerosols, ozone, water vapour and the surface reflective properties.
- Data quality control and assessment: Input quality control, regular benchmarking against ground stations, regular monitoring of consistency and detecting possible trends
- Availability: https://ads.atmosphere.copernicus.eu/datasets/cams-solar-radiation-timeseries for time series at user-defined locations of interest and including the expert mode with detailed access to inputs used https://ads.atmosphere.copernicus.eu/datasets/cams-gridded-solar-radiation for a pre-calculated gridded dataset in 15 min and 0.1° latitude/longitude grid
- Data policy: This dataset is released for use under the CC-BY licence. Highlights and key features of the licence are provided at https://creativecommons.org/licenses/by/4.0/. Full legal text is provided at https://creativecommons.org/licenses/by/4.0/legalcode.Documentation: Dataset information at https://ads.atmosphere.copernicus.eu/datasets/cams-solar-radiation-timeseries?tab=overview

  User‘s Guide accessible via https://ads.atmosphere.copernicus.eu/datasets/cams-solar-radiation-timeseries?tab=documentation

  Quarterly validation reports at https://atmosphere.copernicus.eu/supplementary-services

2.3. How to cite CAMS Radiation Service data

In addition to the requirements of the applicable license(s), users must:

- cite the ADS catalogue entry;
- provide clear and visible attribution to the Copernicus programme
- attribute each data product used by citing the relevant original literature

Citing the ADS catalogue entry

Copernicus Atmosphere Monitoring Service (2020): CAMS solar radiation time-series. Copernicus Atmosphere Monitoring Service (CAMS) Atmosphere Data Store, DOI: 10.24381/5cab0912 (Accessed on DD-MMM-YYYY)

Copernicus programme attribution

[Generated using/Contains modified] Copernicus Atmosphere Monitoring Service information [year]. Neither the European Commission nor ECMWF is responsible for any use that may be made of the Copernicus information or data it contains.

Citing the CAMS radiation service's original scientific literature

Schroedter-Homscheidt, M., Azam, F., Betcke, J., Hanrieder, N., Lefèvre, M., Saboret, L., Saint-Drenan, Y.-M.: Surface solar irradiation retrieval from MSG/SEVIRI based on APOLLO Next Generation and HELIOSAT-4 methods, Contrib. Atm. Sci./Meteorol. Z.,2022, doi:10.1127/metz/2022/1132.

Qu, Z., Oumbe, A., Blanc, P., Espinar, B., Gesell, G., Gschwind, B., Klüser, L., Lefèvre, M., Saboret, L., Schroedter-Homscheidt, M., and Wald L.: Fast radiative transfer parameterisation for assessing the surface solar irradiance: The Heliosat-4 method, Meteorol. Z., 26, 33-57, doi: 10.1127/metz/2016/0781,2017. Available for download at https://www.schweizerbart.de/papers/metz/detail/26/87036/Fast_radiative_transfer_parameterisation_for_asses?af=crossref.

Citing the CAMS clear-sky time series' original scientific literature

Gschwind, B., Wald L., Blanc, P., Lefèvre, M., Schroedter-Homscheidt, M., Arola, A., 2019. Improving the McClear model estimating the downwelling solar radiation at ground level in cloud free conditions – McClear-V3., Meteorol. Z./Contrib. Atm. Sci., 28, 2, 147-163, doi:10.1127/metz/2019/0946. Available for download at https://www.schweizerbart.de/papers/metz/detail/28/90593/Improving_the_McClear_model_estimating_the_downwelling_solar_radiation_at_ground_level_in_cloud_free_conditions_McClear_v3

Lefèvre, M., Oumbe, A., Blanc, P., Espinar, B., Gschwind, B., Qu, Z., Wald, L., Schroedter-Homscheidt, M., Hoyer-Klick, C., Arola, A., Benedetti, A., Kaiser, J., W., and Morcrette, J.-J.: McClear: a new model estimating downwelling solar radiation at ground level in clear-sky conditions, Atmos. Meas. Tech., 6, 2403–2418, doi: 10.5194/amt-6-2403-2013, 2013. Available for download at http://www.atmos-meas-tech.net/6/2403/2013/amt-6-2403-2013.pdf

3. The legacy methods

3.1. History of the Heliosat methods

The feasibility of extracting the global solar surface irradiance (SSI) from geostationary satellites images like Meteosat was shown by Tarpley (1979) and Möser and Raschke (1984). Very early, the European Commission funded research to develop methods for retrieving the SSI from Meteosat images (Grüter et al., 1986). Among those, the Heliosat method was developed at MINES ParisTech (MPT, Cano et al., 1986). It became very popular and has been adopted by many researchers. Therefore, it underwent many changes aiming at improvements; the versions bearing major improvements were numbered. The legacy methods are numbered Heliosat-1, Heliosat-2, and Heliosat-3 and were based on cloud-index methods. The CAMS Radiation Service nowadays uses Heliosat-4 based on cloud physical parameters. Having noticed frequent confusion about the differences among the versions, this chapter aims at an overview on the different precursor versions ('legacy methods'). To our knowledge there is no other single document describing the scientific evolution of the Heliosat algorithm family in a concise manner.

The principles of the legacy Heliosat methods are illustrated in Figure 3.1. In most cases, a cloud exhibits a larger reflectance than the ground. Consequently, the appearance of a cloud in the field of view of the satellite sensor should result in an increase of the perceived signal: the cloud (target 2) appear brighter (whiter) than the ground (target 1). The magnitude of the difference between both targets is related to the depletion of the downwards radiation by the atmosphere. Of course, the situation where one can compare a cloudy pixel to a neighbour cloud-free pixel rarely happens. Therefore, Heliosat comprises a modelling of the SSI that should be observed by the sensor if the sky were clear for any pixel.

The legacy versions of Heliosat-1/-2/-3 have in common to be divided into two parts regarding the physical modelling: converting the satellite image into a cloud index and converting the cloud index in irradiance. Therefore, they are called cloud index methods.

The original Heliosat method makes use of the clearness index K_T. K_T is defined as the ratio of the SSI to the irradiance received at the top of the atmosphere. It characterizes the depletion of the solar radiation by the atmosphere. The cloud index n is converted into the clearness index by an empirical affine function $K_T = a\ n + b$, whose parameters a, and b, should be derived empirically by comparison with coincident ground measurements. These parameters can be computed for each location of ground station and then spatially interpolated to produce maps of parameters (Cano et al. 1986). They can also be averaged; the mean values are considered valid for a given region, e.g., Europe (Diabaté et al., 1988). Diabaté et al. (1989) observed that for Europe, three sets of parameters were needed: one for morning, one at noon, and one in the afternoon.

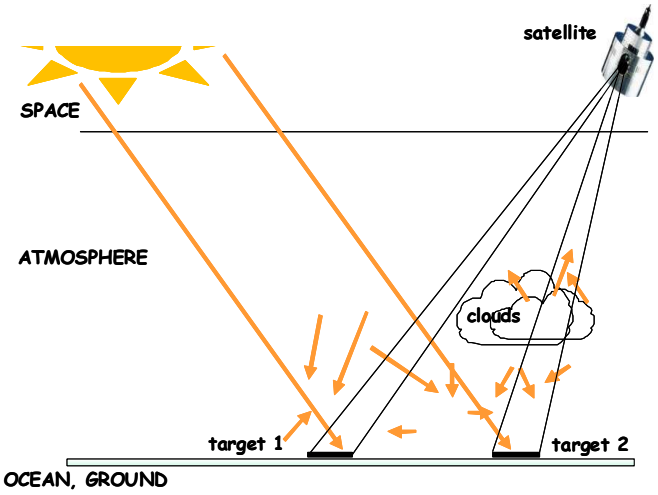

Figure 3.1. Measurement principle as used in cloud-index methods

A delicate part in the legacy Heliosat method is the determination of the cloud-free instants. As Heliosat-1/-2/-3 use only one channel in visible range, the cloud-free instants should be detected by exploiting the time-series. A cloud-free instant should correspond to a minimum in the time-series, provided all other conditions are equivalent, which is not the case; for example, the sun position is changing within the day and also from day to day for the same hour. Espinar et al. (2009) or Lefèvre et al. (2007) found that a relative error in the ground albedo leads to a relative error of the same magnitude in SSI under clear-sky, i.e., a relative error of order 10 % of the SSI in cloudy cases. Another delicate part in cloud-index based methods is the determination of the albedo of the brightest clouds. The error due to an error in this albedo increases as the sky is becoming cloudy; consequently, the relative error in the SSI can be very large, e.g., 60 % (Espinar et al., 2009; Lefèvre et al., 2007).

Beyer et al. (1996) at the University of Oldenburg (Germany) produced a version called later Heliosat-1. It enhanced the original Heliosat method in several aspects. The major one is the adoption of the clear-sky index *Kc* instead of the clearness index K_T. The clear-sky index is defined as the ratio of the actual SSI to the SSI that would be received if the sky were cloud-free. The great advantage of the substitution is that the relationship between *Kc* and *n* is universal and is now: $Kc = 1-n$. It has been found by these authors and confirmed by others that little was lost in quality by adopting this relationship for any part of the world and any time. Further work was done to remove partly the dependence of the received radiance with the viewing angle, thus leading to a more spatially-homogeneous cloud-index. In addition, work was performed on the determination of the ground and cloud albedo. Several empirical parameters used in this determination, e.g., the allowed change in time of the ground albedo or the threshold to detect cloud-free instants were revisited and new values were proposed to better account for actual measurements of SSI made by European ground stations.

To improve the accuracy and the reliability of the estimation and to facilitate the implementation of the method, Rigollier et al. (2004) designed the Heliosat-2 version at MINES ParisTech. It exploits the advances proposed by Heliosat-1 and seeks at removing empirical parameters. This is done by adopting several models that have been published independently of Heliosat or Meteosat. This requests a calibration of the Meteosat images to convert gray values into radiances and then reflectances. The clear-sky model proposed in the European Solar Radiation Atlas (ESRA) was adopted (Rigollier et al., 2000). This Heliosat-2 version is presented hereafter.

The Heliosat-3 version has been designed in a collaborative EU-funded project led by University of Oldenburg, and comprising MINES ParisTech and DLR among others. It is characterized by a clear-sky model, called SOLIS, which is an approximation of radiative transfer equations for fast implementation (Mueller et al. 2004) which is coupled to the cloud-index approach.

3.2. Overview of the Heliosat-2 method

The irradiance I for an instant t and location (x, y) is equal to

$$I(t, x, y) = I_c(t, x, y)\, K_c(t, x, y) \qquad (3.1)$$

where $I_c(t, x, y)$ is the irradiance for the clear-sky case; $K_c(t, x, y)$ is called the clear-sky index, is positive, and quantifies the depletion of I_c due to clouds. Thus, the method is based on *1)* a model of irradiance for clear-sky whose results are more or less depleted as a function of the cloud properties to yield actual irradiance. This concept is the basis of many published models outside Heliosat-2 (Rigollier et al., 2004).
The clear-sky index $K_c(t, x, y)$ is computed from the analysis of the Meteosat image at instant t and from the time-series of images prior to the current one. A cloud-index $n(t, x, y)$ is defined:

$$n(t, x, y) = [\rho(t, x, y) - \rho_g(t, x, y)] / [\rho_{cloud}(t, x, y) - \rho_g(t, x, y)] \qquad (3.2)$$

where ρ, ρ_{cloud}, and ρ_g are the reflectances respectively observed by satellite for the pixel under concern, the brightest clouds, and the ground. The cloud index is close to 0 when the observed reflectance is close to the ground reflectance, i.e., when the sky is clear. It can be negative if the sky is very clean, in which case ρ is smaller than ρ_g. The cloud index increases as the clouds are appearing. It can be greater than 1 for clouds that are optically very thick.

An empirical relationship was derived from coincident ground measurements and Heliosat-2 results that links n to K_c (Figure 3.2):

$$\begin{aligned} &n < -0.2 && K_c = 1.2 \\ &-0.2 < n < 0.8 && K_c = 1 - n \\ &0.8 < n < 1.1 && K_c = 2.0667 - 3.6667\, n + 1.6667\, n^2 \\ &n > 1.1 && K_c = 0.05 \end{aligned} \qquad (3.3)$$

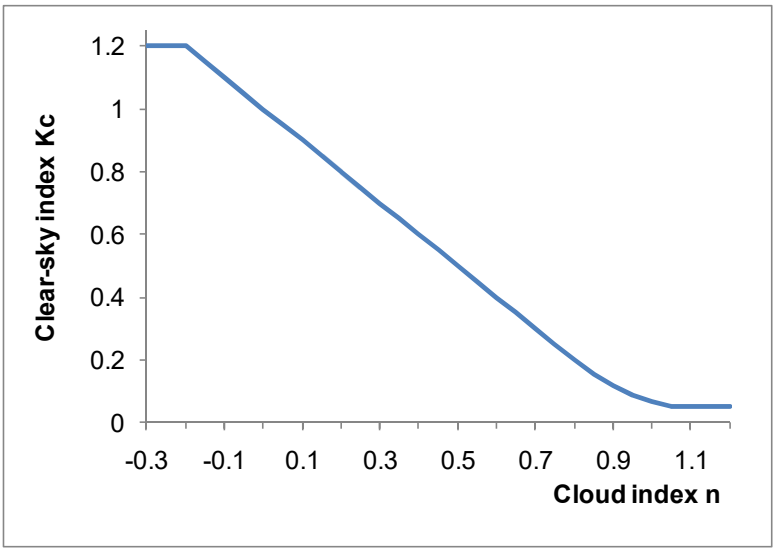

Figure 3.2. Relationship between the cloud index n and the clear-sky index Kc

For the computation of the BNI (beam or direct normal irradiance) in the SOLEMI database, the following equation is used:

$$BNI = BNI_{clear} * exp(a\ n) \qquad (3.4)$$

where a is a number which depends on the viewing geometry, the brightness temperatures in thermal infra-red of the pixel, and the spatial variability in the cloud index.

The model of irradiance for clear-sky used for HelioClim is that of the European Solar Radiation Atlas (ESRA); the clear-sky model for SOLEMI (Hoyer-Klick et al., 2016) is the model of Bird (Bird and Hulstrom, 1981) as later been modified by Iqbal (1983) as Model C. Their inputs are discussed in further sections.

There are limitations in the implementation of this concept. One major limitation is that $I_c(t, x, y)$ is unknown. Knowledge on aerosols and other influencing atmospheric parameters is too poor to permit to retrieve on an operational basis the irradiance $I_c(t, x, y)$ for any time and any location. Therefore, the best that can be provided is a typical value of $I_c(t, x, y)$ for this instant and location. In order to cope with that uncertainty, the clear-sky index $K_c(t, x, y)$ is allowed to be greater than 1 while it should not in principle.

The current method Heliosat-2 does not account for the sudden appearance of snow; large errors may appear in the presence of snow cover in cloud-free atmosphere.

3.3. Inputs to clear-sky models

3.3.1. Aerosols

Aerosols have the strongest influence on clear-sky irradiances through absorption and scattering processes. Modelling aerosols in the atmosphere is very difficult and is one of the major current tasks in atmospheric and climate research. The sources of aerosols are highly variable in space and in time. The interaction of the aerosol particles with the atmospheric trace gases and clouds is complex; the life time is rather short. Models are making good progress in capturing aerosol evolution, but the characterization of the sources is still difficult. Current state-of-the-art data sets currently include satellite observations of aerosols, precursor trace gases, clouds and precipitation and networks of surface-based instruments assimilated into a chemical transport model.

Chemical transport models take aerosol processes as an integral part within the simulation scheme and make use of satellite data. Earlier used datasets have been developed as offline models for the use in climate models (Tegen et al. (1997), Kinne et al., 2006, Collins et al., 2001; Zender et al., 2003), but in the CRS an online chemical transport model with data assimilation and coupled to a numerical weather prediction model is now used.

3.3.2. Water vapour

Water vapour mainly absorbs the solar irradiance in the thermal spectrum and has a larger influence than ozone. The legacy databases used the NCEP/NCAR-Reanalysis of the Climate Diagnostic Center (CDC-NOAA) with a spatial resolution of 2.5° x 2.5° while the CRS now is fully coupled to a numerical weather prediction model in a spatial resolution of 40 km.

3.3.3. Ozone

Ozone absorbs the irradiance predominantly at wavelength lower than 0.3 µm. Therefore, the extinction of ozone is fairly low for the complete solar spectrum. A data set from the Total Ozone Mapping Spectrometer (TOMS) sensor was used (McPeters et al., 1998) in the legacy databases while the CRS now uses the ozone field as modelled in the chemical transport model used in CAMS.

3.3.4. Linke Turbidity

The Linke turbidity factor (TL, for an air mass equal to 2) is a very convenient approximation used in many models in the solar energy community. It describes the optical thickness of the atmosphere due to both the absorption by the water vapour and the absorption and scattering by the aerosol particles relative to a dry and clean atmosphere. A worldwide database for TL has been proposed by Remund et al. (2003) and was used in the precursor services.

One may use the CAMS Clear Sky service to obtain Linke Turbidity Factors from CAMS output. Knowing the clear sky direct irradiance and the extra-terrestrial irradiance, the Lambert-Beer relation can be used to derive an effective optical thickness of a non-dry/non-clear but cloud-free atmosphere this can be used in the definition equation for Linke Turbidity as given e.g. in eq. 9 in Hammer et al. (1998) or in Ineichen and Perez (2002).

3.3.5. Known problems with input data in the legacy databases

Aerosol loading and water vapour amount are difficult to measure with remote sensing methods over land. Thus, aerosols and water vapour data are usually taken from numerical model reanalyses and the accuracy and resolution are limited. These data have often been available only on a daily or monthly basis and with a resolution close to 1° or coarser in the legacy databases. The poor availability of accurate inputs is a recurrent problem. The CAMS Service provides these inputs by the means of the ECMWF/CAMS IFS model suite. The integration of CAMS clear sky parameters is a major step forward from the legacy processing chains towards the CAMS Radiation Service.

Empirical models have to make simplifying assumptions to transform the cloud information derived by the satellite into an effective cloud transmission. The applied function for a visible cloud index as e.g. in Figure 3.4 may not be the best for all sites and climatic conditions.

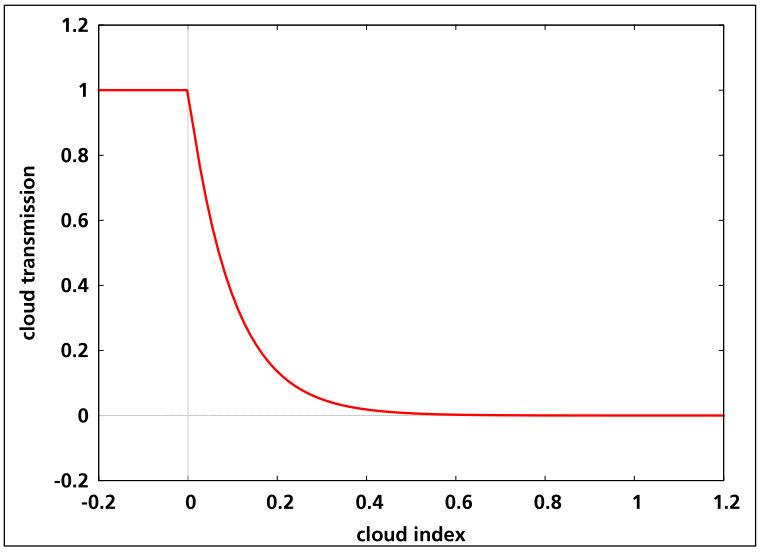

Figure 3.4. Example of transfer function from cloud observation (cloud index) to cloud transmission.

4. The Heliosat-4 method

Compared to the legacy methods Heliosat-1/-2/-3 and the legacy databases HelioClim-3 and SOLEMI, the CAMS Radiation Service makes now use on a physical retrieval of cloud parameters and a fast parameterization of radiative transfer in the Heliosat-4 method.

The Heliosat-4 method (Qu et al., 2016) estimates the down-welling shortwave irradiance received at ground level in all sky conditions. It provides global irradiance and its direct and diffuse components on a horizontal plane and direct irradiance for a plane normal to sun rays. It is a fully physical model using a fast, but still accurate approximation of radiative transfer modelling and is therefore well suited for geostationary satellite retrievals. It is composed of two models based on abaci, also called look-up tables: the McClear (Lefèvre et al., 2013; Gschwind et al., 2019) model calculating the irradiance under cloud-free conditions and the McCloud model calculating the extinction of irradiance due to clouds. Both have been realized by using the libRadtran (Mayer and Kylling, 2005) radiative transfer model.

The main inputs to Heliosat-4 are aerosol properties, total column water vapour and ozone content as provided by the CAMS global forecast and reanalysis services every 3 h (Benedetti et al., 2009; Morcrette et al., 2009; Inness et al., 2019; Remy et al., 2019). Cloud properties are derived from images of the Meteosat Second Generation (MSG) satellites in their 15 min temporal resolution using the APOLLO_NG (Klüser et al., 2015) scheme. The use of cloud parameters is further described in Qu et al. (2016) and from CAMS v4.0 onwards the use of cloud properties is extended by a circumsolar radiation parametrisation as described in section 4.4. Please note that from CAMS v4.0 onwards APOLLO_NG replaces the previously used APOLLO cloud retrieval package (AVHRR Processing scheme Over cLouds, Land and Ocean, Kriebel et al., 1989; Kriebel et al., 2003).

4.1. Concept of Heliosat-4

The Heliosat-4 method is based on the decoupling solution proposed by Oumbe et al. (2014). They have shown that in the case of infinite plane-parallel single- and double-layered cloud, the solar irradiance at ground level computed by a radiative transfer model can be approximated by the product of the irradiance under clear atmosphere and a modification factor due to cloud properties and ground albedo only. Changes in clear-atmosphere properties have negligible effect on the latter so that both terms can be calculated independently.

Let G denote the global SSI for any sky. G is the sum of the beam component B of the SSI – also known as the direct component– and of the diffuse component D, both received on a horizontal surface. Let note G_c, B_c and D_c the same quantities but for clear-sky. The ratios K_c and K_{cb} are called clear-sky indices:

$$K_c = G / G_c \qquad (4.1)$$
$$K_{cb} = B / B_c$$

K_c is also called cloud modification factor in studies on UV or photosynthetically active radiation. The indices K_c and K_{cb} concentrate the cloud influence on the downwelling radiation and are expected to change with clear-atmosphere properties P_c since the clouds and atmospheric constituents are mixed up in the atmosphere. Eq. 9.1 can be expanded:

$$G = G_c(\theta_S, \rho_g, P_c)\, K_c(\theta_S, \rho_g, P_c, P_{cloud}) \qquad (4.2)$$
$$B = B_c(\theta_S, P_c)\, K_{cb}(\theta_S, P_c, P_{cloud})$$

where

- Θ_S is the solar zenithal angle,
- ρ_g the ground albedo,
- P_c is a set of 7 variables governing the optical state of the atmosphere in clear-sky: *i)* total column contents in ozone and *ii)* water vapour, *iii)* elevation of the ground above mean sea level, *iv)* vertical profile of temperature, pressure, density, and volume mixing ratio for gases as a function of altitude, *v)* aerosol optical depth at 550 nm, *vi)* Angström coefficient, and *vii)* aerosol type,
- P_{cloud} is a set of variables governing the optical state of the cloudy atmosphere: *i)* cloud optical depth (τ_c), *ii)* cloud phase, *iii)* droplet effective radius, and *iv)* the vertical position of the cloud.

Oumbe et al. (2014) have quantified the error made in decoupling the effects of the clear atmosphere from those due to the clouds in cloudy sky, i.e. if changes in P_c are neglected in K_c, respectively K_{cb} in Eq. 9.2. This is equivalent to say that the first derivative $\partial K_c / \partial P_c$, resp. $\partial K_{cb} / \partial P_c$, is close to 0. In that case, Eq. 9.2 may be replaced by the following approximation:

$$G \approx G_c(\theta_S, \rho_g, P_c)\, K_c(\theta_S, \rho_g, P_{c0}, P_{cloud}) \qquad (4.3)$$
$$B \approx B_c(\theta_S, P_c)\, K_{cb}(\theta_S, P_{c0}, P_{cloud})$$

where P_{c0} is an arbitrarily chosen but typical set P_c. The error made in using this approximation depends mostly on the solar zenithal angle, the ground albedo and the cloud optical depth and is less than 2% in relative value for most cases. The maximum error (percentile 95%) on global and direct irradiances is less than 15 W m^{-2}. The errors made are similar to those recommended by the World Meteorological Organization for high quality measurements of the solar irradiance.

These results are important in the view of an operational system as it permits to separate the whole processing into two distinct and independent models, whose inputs are different. Each part of the equation can be processed following the available spatial and temporal resolutions of their inputs. This is of practical importance in CAMS. CAMS clear sky parameters are typically provided only every 3 h. Their spatial resolution is 40 km. On the other hand, the cloud properties are derived from the processing of Meteosat images with an APOLLO Next Generation (APOLLO_NG) chain. Such products are available every 15 min for each Meteosat pixel. Therefore, having two different modules for clear-sky and cloudy atmospheres, eases the burden of coping with these differences in resolution and availability.

4.2. Schematic view of the Heliosat-4 method

In Heliosat-4 (Fig. 4.1) two models are used: McClear for the clear-sky (which is defined as being cloud-free) irradiances G_c and B_c, and McCloud for computing the clear-sky indices K_c and K_{cb} in cloudy conditions.

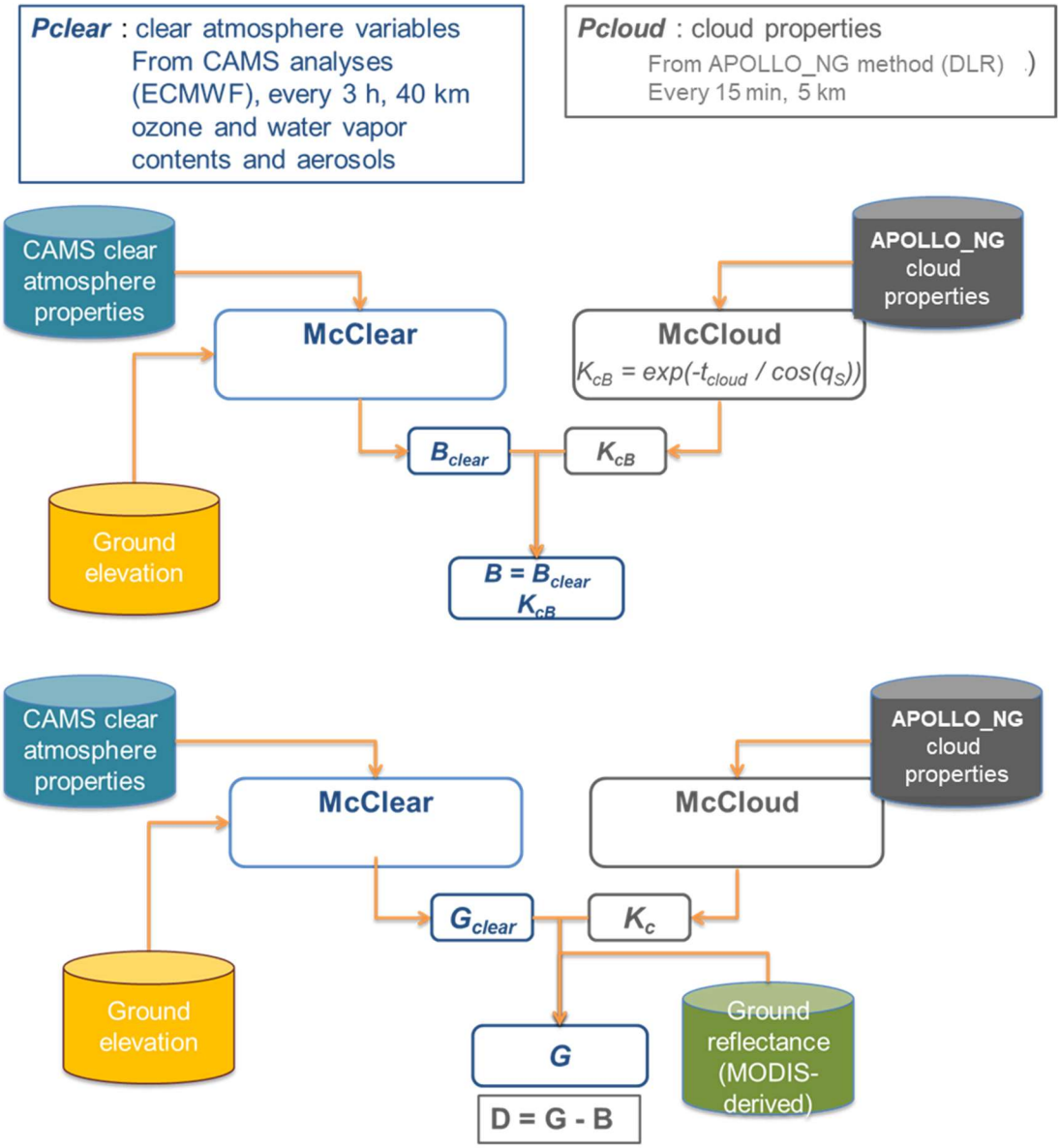

Figure 4.1. Schematic view of the Heliosat-4 method for direct (upper panel), global and diffuse (lower panel) irradiances

4.3. Overview of the McClear model

The fast clear-sky model called McClear (Lefèvre et al., 2013) estimates the downwelling shortwave direct and global irradiances received at ground level under cloud-free skies.

Within the Heliosat algorithm family, cloud-free skies are traditionally named ‘clear sky’ and this terminology is kept even if very turbid conditions in e.g. a dust aerosol event may not appear to be ‘clear sky’.

McClear implements a fully physical modelling replacing empirical relations or simpler models used before (e.g. as described in section 3). It exploits aerosol properties, and total column content in water vapour and ozone produced by the CAMS global service. It accurately reproduces the irradiance computed by the libRadtran reference radiative transfer model with a computational speed approximately 10^5 times greater by adopting the abaci, or look-up tables, approach combined with interpolation functions. It is therefore suited for geostationary satellite retrievals or numerical weather prediction schemes with many pixels or grid points, respectively. Several assessments of the quality of the outputs of McClear v2 have been made (Eissa et al., 2015; Lefèvre, Wald, 2016; Lefèvre et al., 2013; Qu et al., 2014).

Based on the input data availability in the CAMS service, McClear delivers time-series of SSI for any place in the world and any instant starting from 2004.

Several drawbacks have been identified during these assessments and daily operations. Hence, a new version v3 was implemented on 2017-10-11 (Gschwind et al., 2019). Inputs to McClear v3 are:

- θ_S as provided by the fast algorithm for the solar position SG2 (Blanc and Wald, 2012);
- three parameters describing the bidirectional reflectance distribution function (BRDF) in the Moderate-resolution Imaging Spectroradiometer (MODIS) database (Schaaf et al., 2002) from which ρ_g can be computed. The worldwide climatological monthly means of these three parameters as derived by Blanc et al. (2014) from the MODIS BRDF/Albedo model parameters product MCD43C1 and MCD43C2 data have been used. This dataset has a spatial resolution of 0.05°;
- the altitude of the ground level, given by the user, or taken from the SRTM data set (Farr et al., 2004; 30 m resolution) if available or the GTOPO30 data set (Gesch and Larson, 1996);
- the elevation of the CAMS cell above the ground to describe the vertical profile between the CAMS IFS model resolution and the ground level elevation model used;
- the total AOD at 550 nm and the partial optical depths at 550 nm for all aerosol species given by CAMS;
- the total column contents in ozone and water vapour given by CAMS;
- the vertical profiles of temperature, pressure, density, and volume mixing ratio for gases as a function of altitude, which are those from the USA Air Force Geophysics Laboratory (AFGL, Anderson et al. 1986) as implemented in libRadtran: tropics, mid-latitude summer and winter, and sub-Arctic summer and winter. A zoning has been constructed for the

automatic selection of the atmospheric profile for any site based on the Koeppen climate classification map (Lefèvre et al., 2013). In order to avoid spatial discontinuity due to the abrupt change in vertical profiles, the original algorithm of Lefèvre et al. (2013) has been improved. McClear computes G_c and B_c for each profile and averages these estimates weighted by the inverse of the distance of the site of interest to the closest border of each zone. The period ranging from November to April is considered as boreal winter and austral summer.

Compared to McClear v2, McClear v3 removes several discontinuities:

- those induced by abrupt changes in the aerosol mixtures due to the empirical algorithm;
- those in time due to abrupt changes from winter to summer and reciprocally in the adopted atmospheric profiles;
- those with changing solar zenithal angles induced by the piece-wise MLB functions. In addition, McClear v3 has extended the estimation of the diffuse irradiance to solar zenith angle greater than 90°.

4.4. Overview of the McCloud model

The clear-sky index for direct radiation K_{cb} is computed as a function of the cloud optical depth τ_c.

$$K_{cb} = exp[-\tau_c / cos(\theta_S)] \qquad (4.4)$$

K_c is computed by the means of a look-up table approach combined with interpolation functions between the nodes of the tables. Another result from MACC and MACC-II projects is that the vertical position of clouds and their geometrical thickness have a very small effect on *G.* As a consequence, typical altitudes of clouds may be selected instead of updated and localized values. Four types of clouds have been selected as this information is provided by the APOLLO scheme, as described later:

- low cloud: water cloud at low altitude. The cloud base height is 1.5 km and the geometrical thickness is 1 km,
- medium cloud: water cloud at medium altitude. The cloud base height is 4 km with a thickness of 2 km,
- high cloud: water or mixed phase cloud of large vertical extent from low altitude to medium altitude. The cloud base height is 2 km and the thickness is 6 km,
- thin ice cloud: ice cloud with a base height of 9 km and a geometrical thickness of 0.5 km.

High clouds, such as *cumulonimbus* which extend vertically from 1 and 2 km up to the tropopause (8-10 km), are mostly composed by water droplets and may have a cloud top made of ice crystals. They are currently treated as water clouds though it may be advantageous if these clouds are treated as two-phase clouds.

Droplet effective radius is set to typical values of 20 μm for thin ice clouds and 10 μm for water and mixed phase clouds.

Four abaci were constructed containing values of K_c, one for each type of cloud. The node points in an abacus are:

- solar zenithal angle Θ_S (deg): 0, 5, 10, 15, 20, 25, 30, 35, 40, 45, 50, 55, 60, 65, 70, 75, 80, 85, 89,
- cloud optical depth τ_c: 0.1, 0.5, 1, 2, 3, 4, 6, 8, 10, 13, 16, 20, 25, 30, 37, 45, 55, 65, 75, 90, 110, 140, 180, 230, 290, 370, 500,
- ground albedo ρ_g: 0, 0.1, 0.9.

The abaci were computed by running libRadtran with 'DISORT 16 stream' as solver. Inputs to libRadtran were the nodes listed above, and a typical set P_{c0} defining the state of the clear atmosphere:

- the middle latitude summer from the USA Air Force Geophysics Laboratory (AFGL) data sets is taken for the vertical profile of temperature, pressure, density, and volume mixing ratio for gases as a function of altitude,
- aerosol properties: optical depth at 550 nm is set to 0.20, Angström coefficient is set to 1.3, and type is continental average,
- total column content in water vapour is set to 35 kg m^{-2},
- total column content in ozone is set to 300 Dobson unit,
- elevation above sea level is 0 m.

Radiative transfer as used here assumes that clouds are infinite and made of plane-parallel layers. In reality three-dimensional cloud effects as e.g. the parallax effect (Schutgens and Roebeling, 2009; Greuell and Roebeling, 2009) and the overshooting of global irradiances (Schade et al., 2007) are observed. These effects are also very sensitive to the geometrical height, the extension and the overall three-dimensional structure of the cloud, but cannot be treated easily by plane-parallel radiative transfer simulations. Nevertheless, in the operational geostationary satellite-based irradiance retrievals, such input on three-dimensional cloud structures is mostly unavailable. Therefore, these effects are not treated by any parameterization.

In the CAMS Radiation Service, cloud physical properties are provided by APOLLO_NG (APOLLO Next Generation, Klüser et al., 2015) which is an extension of the previously used APOLLO (AVHRR Processing scheme Over cLouds, Land and Ocean; Kriebel, Saunders, and Gesell, 1989; Kriebel et al., 2003). The algorithm was originally developed to exploit data from the AVHRR sensors aboard the polar orbiting series of NOAA satellites, in order to estimate the properties of clouds. It has been adapted at DLR to process images of SEVIRI (Spinning Enhanced Visible and Infrared Imager) instrument aboard the series of Meteosat Second Generation satellites (Qu et al., 2016). APOLLO was further enhanced by a probabilistic cloud mask based on Bayesian cloud tests in the APOLLO_NG method (Klüser et al., 2015).

In the original APOLLO scheme, the cloud detection of each pixel is based on five threshold tests, namely the infrared gross temperature (IGT) test, the spatial coherence (SCT) test, the dynamic visible (DVT) test, the shortwave reflectance ratio (R21), and the brightness temperature difference (T45). The IGT test is sensitive to thick or cold-topped clouds which appear cold in infrared observations. The SCT test interprets high spatial variability in reflectances or brightness temperatures as an indicator of a cloudy situation. The DVT test identifies bright reflecting objects. The R21 test uses a ratio of reflectances in two visible channels as the indicator. The T45 test is sensitive for different spectral patterns of ice crystals and water droplets in 11 and 12 µm channels. When each of these tests indicate a cloud free state, the pixel is classified as cloud free. The R21 and SCT tests are then applied again on the remaining pixels, but with different thresholds. If both tests indicate a cloudy state the pixel is classified as full cloudy. The remaining pixels are classified as partially cloudy. The cloud detection in APOLLO_NG uses the same cloud tests, but in a Bayesian approach, thus the resulting cloud probability is composed of the probabilities of each individual test. The cloud probability is interpreted as a linear transition between physical quantities as reflectances, brightness temperatures or reflectance ratios known as confidently clear and confidently cloudy conditions. The classification into partially and fully cloudy pixels is obsolete by this fuzzy logic approach.

APOLLO_NG provides quantities related to cloud for each pixel (3 km at nadir) and every satellite image (15 min for Meteosat, 10 min for Himawari satellites). Among these quantities, there are a mask of cloud probabilities, τ_c and the type of the cloud as low, medium, and high water/mixed phase or thin ice clouds.

For the derivation of cloud optical thickness, the narrow-band surface albedo for the 0.6 µm channel is set to a fixed value of 0.05 for ocean pixels (Kriebel et al., 1989; Roebeling et al., 2006). For land surfaces, nearby cloud-free land pixels in a 31x31, 49x49 or 63x63 pixel box are analysed. If at least one third of pixels in the box are cloud free, their observed average reflectance is used as a cloud-free background value. If there is no observed average cloud-free reflectance available due to a cloud cover, a constant narrow-band surface albedo of 0.1 is chosen. The cloud-free reflectance mean of the surroundings is then used to derive the COT. Taylor and Stowe (1983) provide anisotropy corrections for various satellite zenith and solar zenith angle ranges and low-level, medium-level, high-reaching and optically thin ice clouds. These are used to convert top-of-atmosphere reflectance to directional-hemispherical reflectance. While water vapour absorption can be neglected in the 0.6 µm channel this is not valid for ozone. Atmospheric absorption is corrected following Koepke (1989) and results in top-of-cloud reflectances. The same corrections are applied to the observed average cloud-free reflectance to derive a surface albedo estimate for the 0.6 µm channel. The ground contribution in top-of-cloud reflectances is then removed to obtain the cloud reflectance (Kriebel et al., 1989) and finally, COT is derived from cloud reflectances by applying a parameterization published by Stephens et al. (1984).

Pyrheliometers as used for the Heliosat-4 validation provide ground-based reference observations of direct (or beam) normal irradiance (BNI). According to WMO recommendations (WMO, 2010) they are operated with an opening half-angle of 2.5°, while

the visible sun disk only has an angle of 0.27°. Therefore, they include part of the circumsolar normal irradiance (CSNI) in the measured BNI. Blanc et al. (2014b) recommend that the solar resource databases should provide the BNI as measured by a pyrheliometer with its 2.5° opening half angle together with the sun shape S, the circumsolar contribution (CSC) or the circumsolar ratio (CSR).

Radiative transfer calculations as realized in libRadtran (Mayer and Kylling, 2005) include by default, only the BNI_{strict}, which is defined as the irradiance being not scattered or absorbed at all. This strict direct irradiance definition results in an underestimation of the forward scattered radiation in BNI when compared to ground observations as scattered radiation from inside the sun disk and from the circumsolar region are neglected. This effect is most prominent in the case of thin cirrus or broken clouds, which constitute a significant amount of circumsolar radiation. The apparent transmission T can be parameterized as $T= exp(-k * COT)$ with the apparent COT modification factor k. This factor k describes the difference between the beam radiation (following Beer's law as realized in the radiative transport model) and the part of the scattered inside the solar disk and the circumsolar radiation as observed by the ground instrument. The apparent optical thickness is then defined as $COT_{app} = k * COT$. Quantitative results were obtained for various ground-based observations and reveal values of 0.2 and 0.43 turn as the optimum k on average for optically thick and optically thin clouds, respectively. In the further computation of the SSI and the use of McCloud look-up tables, the apparent COT is used.

4.5. Computation of the SSI

The two first interpolations on θ_S and τ_c provide three values of K_c, one for each ρ_g = 0, 0.1, and 0.9. McClear provides the corresponding three values of G_c. G is computed for each of the three ρ_g:

$$G(\theta_S, \rho_g, P_{c0}, P_{cloud}) = G_c(\theta_S, \rho_g, P_{c0})\, K_c(\theta_S, \rho_g, P_{c0}, P_{cloud}) \qquad (4.5)$$

Let note K_T the clearness index, also called global transmissivity of the atmosphere, or atmospheric transmittance, or atmospheric transmission, defined as:

$$K_T = G / E_0 \qquad (4.6)$$

where E_0 denotes the irradiance received on a horizontal surface at the top of atmosphere for the location and time under concern. The formula of Vermote et al. (1997):

$$K_T(\rho_g) = K_T(\rho_g=0)/ (1 - \rho_g\, S_{cloud}) \qquad (4.7)$$

describes the change in KT as a function of the ground albedo ρ_g and the spherical albedo S_{cloud} of the cloudy atmosphere. S_{cloud} is unknown and in principle, it can be computed using Eq. 9.7 knowing $KT(\rho_g)$, or equivalently $G(\rho_g)$, for any value of ρ_g. In practice, it is sufficient to know $E(\rho_g)$ for three values of ρ_g: 0.0, 0.1, and 0.9, and S_{cloud} can be computed for any ρ_g by linear interpolation and extrapolation:

$$S_{cloud}(\rho_g=0.1) = [1 - G(\rho_g=0)/ G(\rho_g=0.1)] / 0.1 \quad (4.8)$$
$$S_{cloud}(\rho_g=0.9) = [1 - G(\rho_g=0)/ G(\rho_g=0.9)] / 0.9$$
$$a = [S_{cloud}(\rho_g=0.9) - S_{cloud}(\rho_g=0.1)] / 0.8$$
$$b = S_{cloud}(\rho_g=0.1) - 0.1\, a$$
$$S_{cloud} = a\, \rho_g + b$$

and finally

$$G(\theta_S, \rho_g, P_c, P_{cloud}) = G(\rho_g=0) / [1 - \rho_g S_{cloud}]$$
$$= G_c(\theta_S, \rho_g=0, P_c)\, K_c(\theta_S, \rho_g=0, P_{c0}, P_{cloud}) / [1 - \rho_g S_{cloud}] \quad (4.9)$$

4.6. Practical implementation

The ground albedo ρ_g is computed in the same way as in Lefèvre et al. (2013). Blanc et al. (2014) created a worldwide climatological complete database containing monthly means of the three BRDF parameters, called *f*iso, *f*vol, and *f*geo (Schaaf et al., 2002). There is one value of each parameter per month which is allotted to the middle of the day of the middle of the month. A linear interpolation yields *f*iso, *f*vol, and *f*geo for each minute of the day.

In the presence of cloud, ρ_g is not the same as that calculated by McClear and must be computed again. The major difficulty is that ρ_g depends upon $D(\rho_g)$ and $G(\rho_g)$ which depend themselves on ρ_g. At this step, B, and accordingly KT_B, are known, and the method proposed by Lefèvre et al. (2013, Eq. 8) can be used to solve the problem. It has been shown that already a cloud probability of 1% should be used as an indicator for switching to the cloudy scheme.

Solar zenithal angle θ_S and extra-terrestrial irradiance E_0 are computed with the SG2 algorithm (Blanc and Wald, 2012) for the middle of the minute.

Aerosol properties, and total column contents of water vapour and ozone in the CAMS Radiation Service are given every 3 h, starting at 00:00 UT. The ordering of interpolation of parameters was found as having a negligible influence on the results (Lefèvre et al., 2013). A bi-linear spatial interpolation in space is applied to compute a time-series of 3 h values for the given location. A further linear interpolation in time is performed yielding time-series of these atmospheric quantities every 1 min. The 1 min temporal resolution has been chosen as it reflects the variability of irradiation due to the solar position sufficiently well.

Cloud type and apparent τ_{cloud} from APOLLO_NG are given every 10 to 15 min for each pixel of the satellite image. The abacus for the cloud reference category is applied. A series of abacus-internal interpolations is performed to yield K_{cB} and K_{cG} for three ρ_g (=0, 0.1, 0.9) for the 1 min that contains the exact instant of the view of the specific pixel.

Finally, all irradiance parameters are computed every 1 min. If needed, they are summed up to the requested temporal output resolution and irradiation of 15 min, 1 h, 1 day, or 1 month.

4.7. Bias correction

Several publications have dealt with the validation of the CAMS Radiation Service. Qu et al. (2016) focused on 15 min global, direct and diffuse irradiations acquired at BSRN sites. Thomas et al. (2016a) performed a similar validation with BSRN sites but for 1 h summarization time and other years. Thomas et al. (2016b) and Marchand et al. (2016) deal with 1 h global irradiation for specific regions, respectively, Brazil, and Oman and UAE. These authors reported that the correlation coefficients between the ground measurements and the estimates are large, in full agreement with the numerous quarterly validation reports in the CAMS. The articles mentioned above report that the relative bias of global irradiance is often positive and large, noting an overestimation by the CAMS Radiation Service v3 and later v3.2. On the contrary, the retrieval of the direct irradiance often showed an underestimation. A bias correction was developed and implemented on 2017-10-11 in CAMS Radiation Service v3. It reduced observed biases significantly.

During the preparation of CAMS Radiation Service v4, the results of an inter-calibration study for polar orbiters (Meirink et al., 2013) were evaluated. Meirink et al. (2013) found a systematic deviation of SEVIRI VIS channels compared to on-board calibration devices as operated for the MODIS instrument. Following these findings, updated SEVIRI visible channel calibration coefficients are made available and their usage reduces previously observed biases in irradiance components significantly. Further bug fixes were implemented when setting up CAMS Radiation Service v4. Based on all these improvements the bias correction shows very small positive impact and even some unwanted shifts in the distribution of occurring SSI values. **Therefore, the bias correction was omitted from CAMS Radiation Service v4.5 onwards.**

5. Known problems in the retrieval of the SSI

Radiative transfer in the atmosphere is a complex phenomenon. In an operational method for the assessment of the SSI, methods should run fast at the expenses of the complexity of the models and therefore of the accuracy of the retrieved SSI. For example, several interactions between radiation and ground (e.g. reflections on the surrounding slopes) or clouds (reflections on the sides of clouds, multi-layered clouds, etc.) are currently not taken into account.

5.1. Sub-pixel phenomena

There will be an error when the actual conditions differ from the average state. The frequency (15 min) of satellite observations is very satisfactory to describe the transitional phenomena such as convection even if only a snapshot is taken. But the size of the pixel is not adapted to the micro-meteorology. There is a spatial integration which smooths the phenomena. Meteosat pixels have actually an elliptic shape and their average diameter ranges from 3 km to 7 km depending on the viewing geometry of the satellite. The resolution at the sub satellite point is 3 km at ground. Figure 5.1 shows a typical Meteosat Second Generation pixel with N-S extent of about 5 km and E-W extent of about 4 km in Central Europe. In this example, one can note the presence of clouds in the ellipse, whose size is much lower than the pixel size.

Figure 5.1. Typical satellite pixel in Europe with sizes of about 4x5 km².

Rapid changes in cloud cover can be noticed in ground measurements, especially at 1 min sampling steps. The spatial heterogeneity resulting from a patchwork of scattered clouds (e.g. cumulus) may induce a characterisation as cloud free by APOLLO/SEV because of the spatial integration effect.

5.2. Change in terrain elevation within a grid cell in databases

The computation of the SSI from satellite images calls upon a digital terrain model (DTM) whose cell size fits that of the pixel. Actually, the CAMS Radiation Service asks the user for the altitude of the site. If the information is not provided, then three different DTMs are

exploited. This is permitted because the computation is performed on-the-fly. If the site of interest is covered by the DTM SRTM with a spatial resolution of approximately 30 m, then SRTM is used. If not, the DTM GTOPO30 with a resolution of 0.5' of arc angle is used. If not, the DTM TerrainBase (TerrainBase 1995) whose cell size is 5' of arc angle, i.e. approximately 10 km at mid-latitude, is exploited.

In very steep relief, irradiance additionally depends upon cast shadows on the site by surrounding obstacles (Figure 5.2) and not only on the change in altitude.

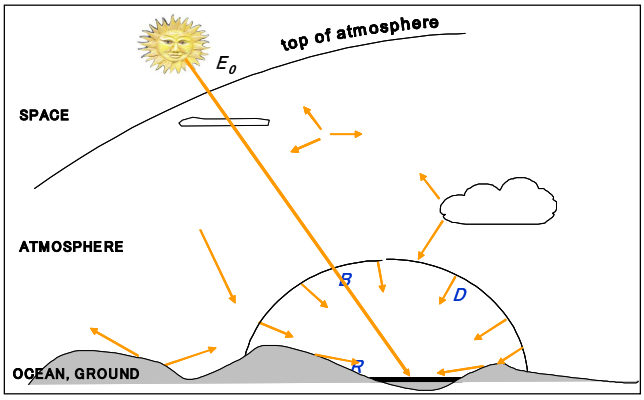

Figure 5.2. Incident irradiance in a complex terrain. B: direct irradiance; D: diffuse irradiance; R: irradiance reflected by nearby terrain

Figure 5.2 shows that the SSI on a horizontal surface is composed of the direct irradiance, diffuse irradiance partly masked by the surrounding mountains, and a reflected part R due to the reflexion on the surrounding slopes. Most often, if not always in operational methods, R is not accounted for; the irradiance calculations are done under the assumption of a flat terrain within the pixel. This applies also for the CAMS Radiation Service. In that case, the tilt angle α and azimuth angle β of the element receiving the radiation are set to 0 and the cosine of the local incident angle θ is:

$$\cos\theta(0,0) = \cos\omega \cos\delta \cos\phi + \sin\delta \sin\phi \qquad (5.1)$$

where ω is the hour angle, δ is the solar declination, and ϕ is the latitude of the site.
In case of non-flat pixel, for each element (*dx, dy*) within a pixel, the cosine of the local incident angle θ is:

$$\cos\theta(\alpha, \beta) = (\cos\omega \cos\delta \cos\phi + \sin\delta \sin\phi) \cos\beta + \cos\omega \cos\delta \sin\phi \cos\alpha \sin\beta + \sin\omega \cos\delta \sin\alpha \sin\beta - \sin\delta \cos\phi \cos\alpha \sin\beta \qquad (5.2)$$

where α and β correspond to the direction of the local slope, respectively in azimuth and tilt. Thus, the SSI of the pixel should be modified by the ratio *R'*:

$$R' = \iint_{pixel} \cos\theta(\alpha(x, y)),\beta(x, y)) \, dx \, dy \, / \cos\theta(0,0) \qquad (5.3)$$

5.3. Coastal sites

Similar to the effect as described in section 5.1 and 5.2, any coastal site may be affected by the inhomogeneity inside the satellite pixel. Such cases are mixed pixels with parts of land and parts of ocean surface and may be misclassified as a cloud. Different thresholds are applied over open sea water than over land as open sea water is typically darker than land surfaces and also than shallow water close to the coast. In the next software version, a filter will be implemented that treats shallow water like land surfaces to better avoid coastal clouds.

5.4. Satellite viewing angles larger than 60°

Retrieval quality degradation with respect to cloud properties is caused by large satellite viewing angles. Locations close to the maximum field of view of MSG are typically on the very edge of the valid domain of the cloud retrieval scheme APOLLO/SEV. The plane-parallel approximation of radiative transfer is not valid anymore and errors due to the parallax effect become important (Schutgens and Roebeling, 2009; Laguarda et al., 2020). The parallax effect shifts the clouds actually covering the site northwards (in the northern hemisphere) and the sensor aboard the satellite does not see the actual atmospheric conditions along the exact optical path between the sun and the station of interest. Additionally, the cloud is seen from the side which contrasts with the plane-parallel assumption made. The quality of cloud physical properties is especially reduced when the sun is low above horizon, e.g. in wintertime, or in early morning and late afternoon. Also, the automatic surface snow/cloud differentiation is more likely to fail. Nevertheless, it has been decided to provide the data in those regions even if large biases are expected as several users have applications where the drawbacks are acceptable. The stations Florianopolis (Brazil) and Toravere (Estonia) are used in the regular quarterly validation reports to quantify this effect.

5.5. Bidirectional reflectance and albedo

Reflexion properties of the ground are a function of the incident and viewing angles. Up to now, these parameters are not operationally available in a high temporal resolution. The CAMS Radiation Service e.g. makes use of monthly maps.

Figure 5.3 shows the angular variation of the reflectance of a coniferous forest in the near infrared (Oumbe 2009). The change in reflectance with the angles can be large; it is greater than 0.1 in Figure 5.3. It can be much larger in the specific case of oceans, where the reflectance depends also on wind speed and varies from values close to zero to values greater than cloud reflectance (Lefèvre et al., 2007). By considering the hemispherical albedo instead of the bidirectional reflectance, one commits a significant error on the part of irradiance reflected by the ground then backscattered by the atmosphere, thus contributing to the diffuse fraction of the SSI. This omission is very often made for operational reasons because of the lack of data describing the ground.

A similar effect can be found in case of clouds because cloud reflectance changes with illuminating and viewing angles due to both the scattering phase function of the cloud and a

viewing geometry from the side on the cloud. This is statistically corrected in APOLLO, but may not be valid in a specific case.

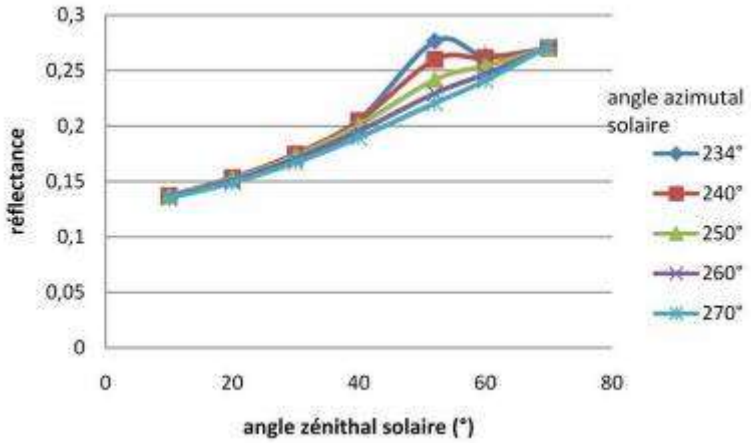

Figure 5.3. Example of variation in ground reflectance with the solar zenithal angle. Viewing and azimuthal angles are set to 52° and 234°, respectively.

5.6. Cloud vertical position and parallax effects

Clouds are located at different altitudes in the atmosphere. If the viewing angle is large, i.e. far from the satellite nadir, the parallax effect becomes noticeable for not too vertically extended clouds at medium and high altitudes. This results in an erroneous assessment of the geographical position of the cloud. The cloud will be assigned to a pixel farther from the nadir of the sensor than the actual one. The pixel over which the cloud is actually located will be seen as a cloud-free pixel and the SSI assessment will be inaccurate. In the individual case, the vertical position of the cloud top and bottom is not known exactly enough to allow a parallax correction. Mean values could be assumed, but have not proven to be successful in the whole MSG field of view and for the MSG multispectral pixel resolution. Therefore, Heliosat-4 does not perform any parallax correction.

5.7. Systematic biases if comparing against BSRN ground observations

The Baseline Surface Radiation Network (BSRN, Ohmura et al., 1998) is frequently used as validation database for irradiances. The spectral range of instruments used in the BSRN network is 285 to 2800 nm for pyranometers of Kipp & Zonen and 295 to 2800 nm for those of Eppley. This is slightly different from the spectral range in Heliosat-4 which is 240 to 4606 nm following Kato et al. (1999). According to simulations performed with libRadtran, this difference in spectral range induces a bias of 3-8 W m^{-2} in GHI, i.e. an overestimation by Heliosat-4.

This spectral difference affects Heliosat-4 through the McClear model. Specific abaci were constructed to create a specific, non public, version of McClear v3 that delivers irradiances for the limited range [285, 2800] nm. This version is used for specific validation usages for scientific publication, control and monitoring of the CRS.

6. The CAMS Radiation Service

6.1. The operational chain

Satellite-data reception at DLR is performed with two independent antenna systems and a daily synchronization is performed to update the rolling archive at DLR. A near-real-time 'online' processing chain is operated to generate satellite-based cloud retrievals. As soon as all input satellite raw data is received in the APOLLO_NG processing is performed at DLR and output is delivered to Vaisala. Since 2022 a similar processing chain is operated at Vaisala premises as primary processing chain to increase service reliability. Within 24 hours further input data as water vapour, ozone, and aerosol properties from the CAMS global forecast and reanalysis services are obtained. First, they consist of forecasted values, which will be replaced by (re-)analysis information as soon as this is available.

Table 6.1. Input data to the CAMS Radiation Service Heliosat-4 method

Variable	Data sources	Temporal resolution	Spatial resolution
Aerosols properties and type	CAMS	3 h	0.4°
Cloud properties and type	APOLLO_NG (DLR)	10 to 15 min	2 to 10 km
Total column content in ozone	CAMS	3 h	0.4°
Total column water vapour content	CAMS	3 h	0.4°
Ground albedo	MODIS (MPT)	Climatology of monthly values	6 km
Solar geometry	SG2 library	1 min	location of interest

At the end of each calendar month, the 'offline' processing chain for satellite-based cloud retrievals aims at filling any gaps which may have occurred in the online processing chain.

McClear service currently uses AOD, ozone and water vapor databases from several sources:

- CAMS Reanalysis from 2004 to 2020 (Iness et al., 2019, AODs, ozone, and water vapour on a 40 km grid, IFS cycle 32R1 and updates as listed in https://confluence.ecmwf.int/display/CKB/CAMS%3A+Reanalysis+data+documentation#CAMS:Reanalysisdatadocumentation-TheIFSmodelanddataassimilationsystem)
- CAMS near real time analysis for 2021 onwards (Morcrette et al., 2009; Benedetti et al., 2009; using IFS Cycle 47r1 or later cycles on a 40 km grid, with updates listed at https://confluence.ecmwf.int/display/CKB/CAMS%3A+Global+atmospheric+composition+forecast+data+documentation#CAMS:Globalatmosphericcompositionforecastdatadocumentation-TheIFSmodelanddataassimilationsystemconfigurations(47r3))

6.2. Description of the CAMS Radiation Service Information System

Given the experience gained by several precursor services delivering databases and applications relating to solar radiation, the CAMS Radiation Service Information System has been designed as a series of Web services that disseminate the products.

These Web services follow the GEOSS (Global Earth Observation System of Systems) standards for interoperability and therefore can be exploited by any GEOSS-compliant portal. This ensures a wide dissemination, more efficient than establishing a specific Web site.

In more details, the system is based on the technologies recommended by the EU-funded MESoR project, the International Energy Agency Task SHC-36, and the GEOSS Architecture Implementation projects, in order to reduce the amount of technological development and to benefit from the adopted standards. The basic concept is the following:

- products from the CAMS Radiation Service can be accessed through the CAMS Atmosphere Data Store,
- each CAMS Radiation Service Web service is an application that can be invoked through the Web using GEOSS standards,
- the CAMS Radiation Service Web services are deployed on the energy community portal (webservice-energy.org) from which they can be executed,
- the CAMS Radiation Service Web services are described in existing catalogues to increase their visibility,
- invoking a CAMS Radiation Service Web service can be done only if the user is registered in the user database of the CAMS Radiation Service and has signed the Licence terms for CAMS Products and Services,
- benefit from the interoperability capability of the CAMS Radiation Service Web services in order to increase their visibility in the CAMS Atmosphere Data Store, on the collaborative SoDa Service platform, in GEOSS-compliant catalogues, and any other interoperable portal or application.

6.2.1. The CAMS Radiation Service Information System as a GEOSS component

Figure 6.7 depicts the infrastructure and its integration as a GEOSS component. Users may request for time-series of radiation values from a web site, shown on the left. In this example, the SoDa Service is shown and is one of many possible clients. It hosts a client: the CAMS Radiation Service Client, which is the interface to the users, collects inputs for time-series, such as location and period, and delivers time-series. The SoDa Service does not connect directly to the CAMS Radiation Service application. An intermediate has been set-up in order to ensure interoperability and facilitate exploitation of CAMS Radiation Service results by other clients. This intermediate is a Web service, more exactly a Web Processing Service (middle of the figure). It receives the request from the CAMS Radiation Service Client, makes itself queries to the CAMS Radiation Service operational system, and flows the resulting time-series to the client.

To ensure a wide dissemination, the CAMS Radiation Service information system is declared as a GEOSS component by registering the component Web Service in a thematic catalogue on energy, itself registered in the GEOSS Components and Services Registry (GEOSS CSR box in the lower right part in Figure). By this means, anyone may discover the CAMS Radiation Service Web Service and will be supplied with details on how to exploit it.

Invocation of the CAMS Radiation Service Web Service is done by the means of a client, called CAMS Radiation Service client in the Figure. This client is provided by the CAMS Radiation Service team or may be developed on the user side as well.

The website webservice-energy.org is a GEOSS community portal. It is an initiative of MINES ParisTech / Armines to host web services dedicated to solar radiation and more generally, energy. The website has several web services: Web Map Services, Web Processing Services, obeying OGC (Open Geospatial Consortium) or W3C (World Wide Web Consortium) standards. The W3C standard is abandoned in favour of the OGC standard. Several services have been developed by MINES ParisTech, others by other providers such as DLR.

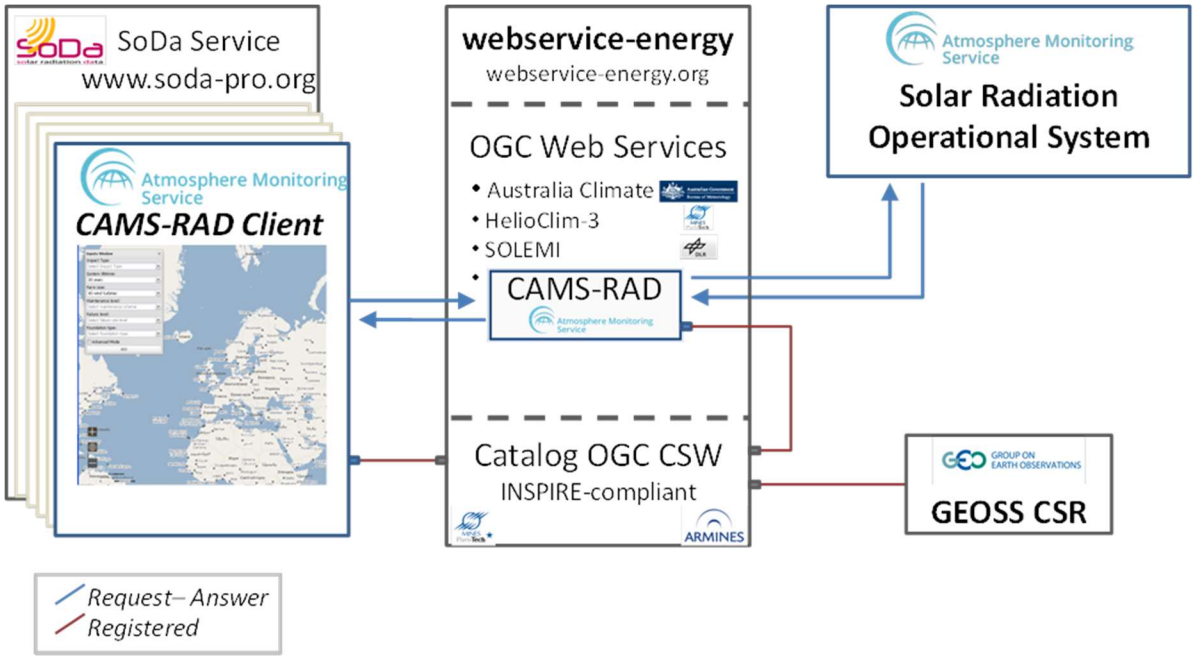

Figure 6.7. Sketch of the CAMS Radiation Service Information System and its integration as a GEOSS component

The website comprises also a catalogue obeying the OGC CSW (Catalogue Service for the Web) standard. The open-source Geonetwork (geonetwork-opensource.org) has been adopted as a CSW tool. Resources are described via metadata that are INSPIRE-compliant (INSPIRE: Infrastructure for Spatial Information in Europe). The catalogue describes the CAMS Radiation Service service, thus enabling its discovery and further exploitation. The catalogue is registered in the GEOSS Components and Services Registry.

6.2.2. Web Processing Service (WPS)

Accessing the CAMS Radiation Service product is done by the means of a Web Processing Service which obeys the standard set up by the OGC and recommended by GEOSS.

The OpenGIS® Web Processing Service (WPS) Interface Standard provides rules for standardizing inputs and outputs (requests and responses) for services aimed at processing the geospatial information extracted from the geographic databases. Here, the CAMS Radiation Service service is defined for the Meteosat field-of-view and the "processing" is the extraction of a time-series for a given location, given period, and summarization.

The standard also defines how a client can request the execution of a process, and how the output from the process is handled. It defines an interface that facilitates the publishing of geospatial processes, their discovery by clients and the linking to those remotely hosted processes. The data required by the WPS can be delivered across a network or can be available through the local server.

WPS defines three operations, two describing service metadata and Input/Output (I/O) characteristics, and a third to execute/run the process:

- getCapabilities: generic WPS instance metadata, list of services in instance,
- describeProcess: full description I/O of service,
- execute: process execution with provided inputs and returned a formatted output, i.e. a netCDF file.

There are several frameworks available to develop and deploy OGC Web Processing Services. Two have been selected configurable application that are released under GNU General Public Licence (GPL) and facilitate the conversion of applications into a Web Processing Service (WPS) in OGC standards. One is the "Toolbox" from the company INTECS, developed in the progress of the Integrated Project (2008-2011) GENESIS funded by the European Commission DG-INFSO under the 7th Framework Programme. The other tool is PyWPS, an open-source project managed by the company Intevation. On the front end, the PyWPS or Toolbox encodes the outputs of the WPS using SOAP and transfers it using HTTP. On the back end, it can be connected via shell scripts to the application, here the CAMS Radiation Service service.

There are two WPS: One is the CAMS Clear-Sky/McClear Radiation service that provides time-series of the SSI that would be observed at any place in the world any time if the sky were clear starting from 2004-01-01. The second WPS is the CAMS Total-Sky Radiation Service that provides time-series of the SSI received at any place in the field-of-view of the Meteosat satellites any time starting from 2004-02-01.

7. The CAMS Radiation Data

7.1. Data policy/Licence

This dataset is released for use under the **CC-BY licence**. Highlights and key features of the licence are provided at https://creativecommons.org/licenses/by/4.0/. Full legal text is provided at https://creativecommons.org/licenses/by/4.0/legalcode.

7.2. Parameters

There are two groups of radiation products (Tab 7.1 to Tab. 7.2) in the CAMS Radiation Service:

- **CAMS Clear-Sky Radiation (McClear) products**: These products describe the clear-sky SSI for the whole world, starting from 2004 and on-going. This product is the result of a numerical atmospheric composition model together with a radiative transfer model and is not based on the processing of any satellite data.

- **CAMS All-Sky Radiation (Heliosat-4) products**: This series describes all skies (cloudy or not) SSI within the MSG field of view, starting from 2004 and on-going. Himawari field of view was added with data from 2016 onwards.

Table 7.1. Main features of the standard time series output products

	CRS-TIME Clear-Sky (McClear method)	CRS-TIME All-Sky (Heliosat-4 method)
ADS name	Cloud-free conditions only	Both cloud-free and actual weather conditions
Type of product	Point data, time-series	
Parameters	GHI, DHI, BHI, BNI	
Geographical area	global	Europe / Africa / Middle East / Atlantic Ocean /Brazil/ east of Asia/ Oceania /Australia (Meteosat Second Generation and Himawari field of view)
Horizontal resolution	Interpolated to point of interest from various spatial input data resolutions	
Time coverage	from 2004-01-01 to (current to -1 day)	from 2004-02-01 for Meteosat and from 2016-01-01 for Himawari field of view to (current – 1 day)
Temporal resolution	1 min, aggregated also to 15 min, 1 h, 1 day, or 1 month Following meteorological standards, the time given for an irradiation value is the end of the integration period.	
Data format	ASCII (CSV), NetCDF	

Data file size	File size depends on the temporal resolution. Largest files are in 1 min temporal resolution and the csv data format (e.g. 60 MB for a 1 year time series in the standard output mode and 10 MB if zipped; 138 MB for a 1 year time series in the expert mode and 19 MB if zipped)
Data access	Atmosphere Data Store, the number of requests is limited to 100 per day (requests are called on SoDa servers). Users are invited to discuss their additional needs with the Copernicus Help Desk individually as the basis for future service evolution.
Processing	on request; data normally available within a few minutes
Update of the databases	1 day delayed mode

Table 7.2. Main features of the standard gridded output products

	CAMS all-sky and clear sky (CRS-GRID) (APOLLO_NG & Heliosat-4 methods)
Type of product	Gridded data
Parameters	GHI, DHI, BHI, BNI
Geographical area	Europe / Africa / Middle East / Atlantic Ocean /Brazil/ east of Asia/ Oceania /Australia (Meteosat Second Generation and Himawari field of view) land and coastal areas only
Horizontal resolution	0.1° in latitude and longitude
Time coverage	from 2005-01-01 to 2023-12-31
Temporal resolution	15 min
Data format	Monthly NetCDF files
Data file size	Depending on region
Data access	Atmosphere Data Store (ADS)
Processing	Pre-processed with CRS version 4.6
Update of the databases	Annually with an approximately 6 month lag

The **period of integration** is defined as the time during which the solar radiation is integrated to yield a period-sum. For example, an integration period of 1 h means that the delivered irradiation is the hourly sum of 1 min irradiation values during one hour.

Following meteorological standards, the time given for an irradiation value is the end of the integration period. For example, the value given for 11:00 means an integration period from 10:00:01 to 11:00:00 if the period is 1 h, or 10:30:01 to 11:00:00 if the period is 30 min.

A **gap handling** is performed automatically:

- The CAMS Radiation Service provides NaN values if large gaps (larger than 1 day) of missing satellite input data exist.

- Shorter gaps of less than a day during daytime are filled with linearly interpolated k_c and k_{cB}. These cases are marked with reliability = 0. These cases mainly occur due to missing satellite raw data.

- In low sun conditions APOLLO_NG does not provide any cloud detection and cloud optical depth. Therefore, the first available k_c value is kept constant for the time between sunrise and this point in time. The same is done in the evening hours – the last available k_c value is kept constant until sunset.

- The reliability index is computed with respect to the amount of 1 minute resolution time slots of the current time summarization (e.g. 15 min or 1 hour) without available cloud information. So, it provides the information how many interpolated cloud time instants are used in the summarization interval.

7.3. CRS - time series datasets

The majority of users stated time series at the location of their interest as their priority. Primary radiation products are therefore time-series of irradiation for a given site and a given period. Once a user request is made via the CAMS Atmosphere Data Store or via scripting, an **on-the-fly processing** is initiated. **It processes the requested time series at the location of interest in the requested duration and temporal resolution. This ensures access to most recent algorithm and input data versions at any time.**

Version numbers are given in the header of each output file and a version history is published at https://confluence.ecmwf.int/display/CKB/CAMS+solar+radiation+time-series%3A+data+documentation#CAMSsolarradiationtimeseries:datadocumentation-Knownissuesandversionupdates.

7.3.1 Detailed info expert output mode

For expert users, all input and output parameters for time series are provided in the '**detailed info expert output mode'**. It can **only** be selected when requesting 1 min resolved time series of up to 1 month length. Besides the standard outputs, it provides:

- Irradiation on horizontal plane at the top of atmosphere
- Clear sky irradiation values GHIc, BHIc, DHIc, and BNIc
- All sky irradiation values GHI, BHI, DHI, and BNI
- Solar zenithal angle for the middle of the summarization (deg)

- Atmospheric profile code: afglus=U.S. standard afglt=tropical afglms=midlatitude summer afglmw=midlatitude winter afglss=subarctic summer afglsw=subarctic winter
- Total column content of ozone (Dobson unit)
- Total column content of water vapour (kg/m2)
- AOD BC. Partial aerosol optical depth at 550 nm for black carbon
- AOD DU. Partial aerosol optical depth at 550 nm for dust
- AOD SS. Partial aerosol optical depth at 550 nm for sea salt
- AOD OR. Partial aerosol optical depth at 550 nm for organic matter
- AOD SU. Partial aerosol optical depth at 550 nm for sulphate
- AOD SO. Partial aerosol optical depth at 550 nm for secondary organics. This quantity was introduced in June 2023 and will have zero values before – indicating unavailability.
- AOD NI. Partial aerosol optical depth at 550 nm for nitrate. This quantity was introduced in July 2019 and will have zero values before – indicating unavailability.
- AOD AM. Partial aerosol optical depth at 550 nm for ammonium. This quantity was introduced in July 2019 and will have zero values before – indicating unavailability.
- Deprecated and replaced by AOD NI: AOD 550. Aerosol optical depth at 550 nm
- Deprecated and replaced by AOD AM: AOD 1240. Aerosol optical depth at 1240 nm
- **Deprecated**, but kept for format consistency: alpha Angstroem coefficient for aerosol. It is set to zero values.
- **Deprecated**, but kept for format consistency: Aerosol type. Type of aerosol: -1=no value 5=urban 7=continental clean 8=continental polluted 9=continental average 10=maritime clean 11= maritime polluted 12=maritime tropical 13=antarctic 14=desert
- fiso. MODIS-like BRDF parameter fiso
- fvol. MODIS-like BRDF parameter fvol
- fgeo. MODIS-like BRDF parameter fgeo
- albedo. Ground albedo
- Cloud optical depth (value of the nearest acquisition time of the pixel is repeated for all minutes, cloud parameters are not interpolated over time, note that the Heliosat-4 algorithm uses kc values interpolated between satellite observations of the cloud)Cloud coverage of the pixel (percentage from 0 to 100, value of the nearest acquisition time of the pixel is repeated for all minutes, cloud parameters are not interpolated over time, note that the Heliosat-4 algorithm uses kc values interpolated between satellite observations of the cloud)

- Cloud type (value of the nearest acquisition time of the pixel, not interpolated over time) -1=no value 0=no clouds 5=low-level cloud 6=medium-level cloud 7=high-level cloud 8=thin cloud
- non-bias corrected all-sky radiation values GHI, BHI, DHI, and BNI (**note: from CRS v4.5 onwards there is no bias correction active anymore, columns are kept for consistency**)

Users may

- make use of this information to establish an extended bias correction based on own localized ground observations;
- use this transparency about all input parameters to run their own solar radiation retrieval schemes;
- contribute easily to evaluation and method development of Heliosat-4 by having access to all input variables;
- develop downstream services by making use on the knowledge on all input parameters e.g. in artificial intelligence methods.

Note should be taken that the content of the detailed info mode may change depending on the version of Heliosat-4 or McClear. Each product contains a detailed description of its content and the user should refer to it.

7.3.2 How to make a request for a CAMS Radiation Service time series

Users need to register for the Atmosphere Data Store with an email and a password. They need to accept the CAMS data policy (section 7.1).

The CAMS catalogue is available at https://ads.atmosphere.copernicus.eu/datasets. Browsing for 'Solar Radiation' provides interactive access to the services on clear-sky and all-sky irradiation in a web-based graphical user interface.

The CAMS Radiation Service is making use of the infrastructure being developed and provided by the SoDa Service (www.soda-pro.com) which is well-known in the solar radiation community which uses it intensively (section 6.3). The 'Solar Radiation time series' provides access to a description of the data set, a form to download the data, and to the documentation and quality control information. The Download data tab provides a simple form to access the services on clear-sky and all-sky irradiation.

To ensure service stability and avoid misuse, a maximum number of time series requests per day and per user is implemented. The number of users reaching this limit is monitored automatically. In case of too many rejected user requests, the hardware will be stepwise enhanced.

Users needing a large number of time series may use the gridded and pre-calculated dataset.

The inputs by users needed to trigger a request for a selected CAMS Radiation Service product are:

- cloud-free conditions only or both cloud-free and actual weather conditions
- the geographical coordinates of the site of interest,
- the elevation of this site above sea-level. By default, the application uses well-known digital elevation models, such as NASA-SRTM.
- the period of time: begin data, end date,
- the summarization, i.e. the period of integration of the SSI, e.g. hourly irradiation.
- time reference
- format

There are two options to perform a data request – either interactively via the CAMS Atmosphere Data Store or via an API request. An example API request can be generated using the online form.

7.3.3 Format of products

7.3.3.1 Data formats

Two formats are provided: CSV (comma-separated values) and binary NetCDF.

The CSV format is a human-readable format, more exactly an ASCII format. Each value is separated from the others by a comma or a semi-column. It can be easily ingested by tools such as Microsoft or OpenOffice suites, Matlab or proprietary applications written in any language (e.g., C, PHP, Python…). Note that it uses English formatted decimal delimiters – on non-English keyboard computers this may cause trouble when reading e.g. in Microsoft Excel or similar tools assuming their local keyboard settings.

In order to follow changes in technology, the NetCDF format has been adopted. NetCDF is a set of software libraries and self-describing, machine-independent data formats that support the creation, access, and sharing of array-oriented scientific data. NetCDF was developed and is maintained at Unidata, part of the University Corporation for Atmospheric Research (UCAR) Community Programs (UCP) in USA. Unidata is funded primarily by the National Science Foundation of USA. It is one of the formats recommended by the GEOSS (Global Earth Observation System of Systems) programme to which is contributing GMES / Copernicus. Several tools are available in the NetCDF Web site to create, handle and exploit NetCDF files (www.unidata.ucar.edu/software/netcdf/).

7.3.3.2 Metadata

Metadata are available to describe the CAMS Radiation Service products in GEOSS-compliant portals. These are *discovery* metadata that permit the cataloguing of these products and therefore to users to discover the products. These metadata obey to INSPIRE

implementation rules (Ménard et al., 2009). As an example, the structure of the CSV files is described – the NetCDF implementation is technically of course different, but the meaning of metadata remains the same.

The CAMS Radiation Service CSV formatted products are organized as lines of values (columns). A set of metadata for exploitation of the data is given above the product columns describing the various features of the products. These metadata are written as text in the delivered file. They conform to the ISO standard where available. Currently these metadata are:

- *title*: title of the time-series, e.g., "CAMS Radiation Service v4.6 all-sky irradiation (derived from satellite data)",
- *content*: a short description of the content of the product, e.g., "A time-series of solar radiation received on horizontal plane and plane always normal to the sun rays at ground level.",
- *provider*: name of the provider
- *date begin, date end*: dates of the beginning and end of the period. The date follows the ISO 8601 standard, e.g. 2004-01-01T01:00:00.000.
- *site latitude and longitude*: geographical coordinates of the site, positive North and positive Earth. The ISO 19115 standard is used,
- *elevation*: elevation above sea level in m,
- *time reference*: time system used: Universal Time (UT), or True Solar Time (TST). This metadata is present only when the period of integration is less than 1 day,
- *summarization*: period during which the energy is summed up to obtain a power average, e.g., 15 min,
- *sampling rate*: period with which the resulting irradiation is sampled. Usually, the sampling rate is set equal to *summarization*,
- *noValue*: the code denoting the absence of value, e.g. NaN (not a number).

The content of each column is described as a free text.
Each line corresponds to an instant of observation. The typical content of a line is:

- instant of observation,
- irradiation at the top of the atmosphere,
- clear-sky irradiation value at ground level, e.g. Clear Sky GHI
- all-sky irradiation value at ground level, e.g., GHI,
- reliability code, ranging from 0 to 1.

The exact content of a line depends on the type of product and the description is provided in the metadata. This is why metadata are included in the file.

7.4. CRS - gridded dataset

There are several options to provide a gridded dataset – any combination of temporal and spatial gridding and any spatial coverage within the satellite field of view is possible as it is a compilation of many individual time series processed and coupled together to generate a gridded dataset. There is no expert mode available for the gridded dataset.

Gridded datasets covering Europe and Africa in a 0.1° latitude/longitude grid and a 15 min temporal resolution were generated with CRS version 4.5 for the period 2005 to 2022. This dataset was updated to CRS version 4.6 and covers now also the Himawari field of view.

Note that this spatial resolution is less than the resolution that can be obtained in the CRS time series mode with individual requests. It is a compromise designed for the usage of large scale data in energy system models and following their user requirements.

8. Validation

8.1. Principles and limitations

The usual way of assessing the quality of retrievals of SSI derived from satellite images is to compare these SSI to coincident measurements performed at ground level. The typical relative accuracy of good quality measurements of the global SSI in the global meteorological network is 4% in terms of root mean square error (WMO, 2012). Therefore, the ground measurements can be seen as an accurate reference against which one may compare the SSI derived from satellite. The comparison is made by computing the difference between the two sets of measurements and analysing statistical quantities such as the bias or the root mean square error.

However, the actual situation is not that simple. Several limitations exist that make the assessment of the quality of retrieved irradiances a very difficult task.

The first limitation is the quality of the ground measurements. Well-maintained stations are rare. Data are often questionable. They should undergo extensive procedures for checking quality. Such procedures are often not enough and a final check must be performed by a trained expert to discard suspicious data.

The time system for acquisition may be universal time, mean solar time, true solar time or local time. However, when stored in a database, there is a conversion in another time system, e.g., universal time. There is consequently a change of original values due to a resampling in time. This resampling can be done using various techniques, usually unspecified. In any case, it is not possible to return to the original values and there is a systematic shift of a fraction of an hour between the two sets of measurements.

The existing standard for hourly data is defined by the WMO (WMO 1981): the time assigned to a data corresponds to the end of the measurement period. For example, hourly data assigned to 11:00 UT has been measured between 10:00 and 11:00 UT. Nevertheless, in several cases the time associated to a measurement represents the beginning, the middle or any instant within the period. This requires resampling at the expenses of decay in quality.

The limitations expressed above due to the time do not hold if one deals with daily, monthly or yearly averages or sums of SSI.

A severe limitation is due to the large differences in principles of measurements. Single point and temporally integrated data (ground measurements) are compared to spatially integrated and instantaneous data (satellite estimates). An assumption of ergodicity (e.g. here equivalence between the temporal and spatial averages) is usually made. This assumption is correct only if the radiation field is spatially homogeneous over an area much larger than a pixel. Other local effects such as reflections on the surrounding slopes or the shadows of clouds may add to the difficulty in comparison.

Perez et al. (1997) and Zelenka et al. (1999) observed the local variability of SSI using measurements made by well-calibrated ground stations close to each other. They found that the variability itself is highly variable from one region to another and it cannot be ignored. Expressing this variability as the ratio of the variance relative to the mean value over the area, they found typical variability in hourly irradiances of 17 % for an area of 10 km in radius. This means that within a 10 x 10 km² area, irradiances measured by a series of similar inter-calibrated sensors would exhibit the same mean value but would differ from hour-to-hour, with a relative variance equal to 17 %. Therefore, observing a relative difference hour-to-hour of 17% between a single pyranometer located in a pixel cannot mean that the satellite-derived irradiances are of bad quality.

The relative variability increases as the surface of the area increases. For example, it typically reaches 25% for a radius of 30 km. It decreases as the time integration increases. For example, it is down to 10% for daily values and a radius of 10 km.

Zelenka et al. (1999) analysed the actual accuracy of satellite estimations of hourly SSI as derived from MSG. They suggest that for a relative deviation of 23% (root mean square error) between ground measurements and satellite estimations, only half of it is due to the estimation method itself. The difference comes from:

- error on the measurements provided by the pyranometer (3 to 5%);
- error due to the spatial variability of solar radiation within the pixel (5 to 8%)
- error due to spatial and temporal heterogeneity of the compared data, e.g. assuming ergodicity (3 to 5%) as discussed above.

8.2. Overview of the validation activities

Outcomes of the CAMS Radiation Service are validated on a regular basis. Three-monthly validation reports can be found at https://atmosphere.copernicus.eu/supplementary-services. In each 3rd quarter, a **multi-annual assessment** is provided as well for each station.

Following current practices in assessment of satellite-derived data in solar energy, the irradiations provided by the CAMS Radiation Service are tested against qualified ground measurements measured in several ground-based stations serving as reference.

The CAMS Radiation Service maintains a **catalogue of stations** providing ground measurements suitable for the validation. This catalogue is updated at least once a year.

Validation should be periodically performed. One of the objectives is to monitor changes in quality from period to period. Once each year, multi-annual statistics are part of the validation reports.

The validation is currently performed at a time step of 1 h for the global, diffuse and direct irradiances. The validation procedure is described in detail in each quarterly validation

report. Each report documents how to cope with different time systems (universal time, true, solar time) and how to take care of the missing data. The procedure comprises two parts. In the first one, differences between estimates and observations are computed and then summarized by classical statistical quantities whose calculations are detailed. In the second part, statistical properties of estimates and observations are compared.

The changes in solar radiation at the top of the atmosphere due to changes in geometry, namely the daily course of the sun and seasonal effects, are usually well reproduced by models and lead to a de facto correlation between observations and estimates of irradiation hiding potential weaknesses. The clearness index is a stricter indicator of the performances of a model regarding its ability to estimate the optical state of the atmosphere. Though the clearness index is not completely independent of the position of the sun, the dependency is much less pronounced than for radiation. Therefore, both irradiation and clearness indices are used.

In addition, the validation of CAMS Radiation Service has been the subject of several scientific articles:

- Mardaljevic J, Brembilla E, Eames M. Daylight solar radiation AMY data derived from satellite remote sensing: Validation against ground measurements and comparison with TMYs. Building Services Engineering Research & Technology. 2025;0(0). doi:10.1177/01436244251335160
- Silvero, C.I., Forciniti, J.D., Medina, F.D., Vega Caro, M. A., Ledesma, R.D.: Comparative Study of Solar Radiation Measurements in Tucuman, Argentina, with Reanalyses and Satellite-Based Datasets, ASME Journal of Solar Energy Engineering, 147, DOI: 10.1115/1.4069864
- Urraca, R., J. Trentmann, U. Pfeifroth, N. Gobron, Can satellite products monitor solar brightening in Europe? Remote Sensing of Environment, 315, 114472, 2024, https://doi.org/10.1016/j.rse.2024.114472.
- Riise, H. N., M. M. Nygard, B. L. Aarseth, A. Dobler, E. Berge, Benchmark of estimated solar irradiance data at high latitude locations, Solar Energy, 282, 112975, 2024, https://doi.org/10.1016/j.solener.2024.112975
- Kenny, D. S. Fiedler, Which gridded irradiance data is best for modelling photovoltaic power production in Germany? Solar Energy, 232, 444-458, doi:10.1016/j.solener.2021.12.044, 2022.
- Mabasa, B.; Lysko, M.D.; Moloi, S.J. Validating Hourly Satellite Based and Reanalysis Based Global Horizontal Irradiance Datasets over South Africa. Geomatics 2021, 1, 429-449. https://doi.org/10.3390/geomatics1040025
- Marchand, M., Al-Azri, N., Ombe-Ndeffotsing, A., Wey, E., Wald, L.: Evaluating meso-scale change in performance of several databases of hourly surface irradiation in South-eastern Arabic Peninsula. Advances in Science and Research, 14, 7-15, doi:10.5194/asr-14-7-2017, 2017.

- Qu, Z., Oumbe, A., Blanc, P., Espinar, B., Gesell, G., Gschwind, B., Klüser, L., Lefèvre, M., Saboret, L., Schroedter-Homscheidt, M., Wald L.: Fast radiative transfer parameterisation for assessing the surface solar irradiance: The Heliosat-4 method, Meteorologische Zeitschrift, 26, 33-57, doi: 10.1127/metz/2016/0781, 2017.
- Schroedter-Homscheidt, M., Azam, F., Betcke, J., Hanrieder, N., Lefèvre, M., Saboret, L., Saint-Drenan, Y.-M.: Surface solar irradiation retrieval from MSG/SEVIRI based on APOLLO Next Generation and HELIOSAT-4 methods, Contrib. Atm. Sci./Meteorol. Z.,2022, doi:10.1127/metz/2022/1132
- Thomas C., Wey E., Blanc P., Wald L., Validation of three satellite-derived databases of surface solar radiation using measurements performed at 42 stations in Brazil. Advances in Science and Research, 13, 81-86, doi:10.5194/asr-13-81-2016, 2016.
- Thomas, C., Wey, E., Blanc, P., Wald, L., and Lefèvre, M.: Validation of HelioClim-3 version 4, HelioClim-3 version 5 and MACC-RAD using 14 BSRN stations. SHC 2015, Istanbul, Turkey, 2-4 December 2015. Energy Procedia, 91, 1059-1069, 2016.
- Trolliet, M., Walawender, J.P., Bourlès, B., Boilley, A., Trentmann, J., Blanc, P., Lefèvre, M., and Wald, L.: Estimating downwelling solar irradiance at the surface of the tropical Atlantic Ocean: A comparison of PIRATA measurements against several re-analyses and satellite-derived data sets, Ocean Science, submitted, 2017.
- Trolliet, M., Walawender, J. P., Bourlès, B., Boilley, A., Trentmann, J., Blanc, P., Lefèvre, M., and Wald, L.: Downwelling surface solar irradiance in the tropical Atlantic Ocean: a comparison of re-analyses and satellite-derived data sets to PIRATA measurements, Ocean Sci., 14, 1021-1056, https://doi.org/10.5194/os-14-1021-2018, 2018.

Several articles focus on the McClear model:

- Lefèvre, M., Oumbe, A., Blanc, P., Espinar, B., Gschwind, B., Qu, Z., Wald, L., Schroedter-Homscheidt, M., Hoyer-Klick, C., Arola, A., Benedetti, A., Kaiser, J. W., Morcrette, J.-J.: McClear: a new model estimating downwelling solar radiation at ground level in clear-sky condition. Atmospheric Measurement Techniques, 6, 2403-2418, doi: 10.5194/amt-6-2403-2013, 2013.
- Lefèvre, M., Wald, L.: Validation of the McClear clear-sky model in desert conditions with three stations in Israel. Advances in Science and Research, 13, 21-26, doi: 10.5194/asr-13-21-2016, 2016.
- Gschwind, B., Wald L., Blanc, P., Lefèvre, M., Schroedter-Homscheidt, M., Arola, A., 2019. Improving the McClear model estimating the downwelling solar radiation at ground level in cloud free conditions – McClear-V3., Meteorol. Z./Contrib. Atm. Sci., 28, 2, 147-163, doi:10.1127/metz/2019/0946.

9. References

Anderson, G. P., S. A. Clough, F. X. Kneizys, J. H. Chetwynd, E. P. Shettle, 1986: AFGL atmospheric constituent profiles (0-120 km), Technical Report AFGL-TR-86-0110, AFGL(OPI), Hanscom AFB, MA. 01736.

Benedetti, A., J.-J. Morcrette, O. Boucher, A. Dethof, R. J. Engelen, M. Fischer, H. Flentjes, N. Huneeus, L. Jones, J. W. Kaiser, S. Kinne, A. Mangold, M. Razinger, A. J. Simmons, M. Suttie, and the GEMS-AER team, 2009. Aerosol analysis and forecast in the ECMWF Integrated Forecast System. Part II: Data assimilation. J. Geophys. Res., 114, D13205, doi:10.1029/2008JD011115.

Benedetti, A., J. W. Kaiser, J.-J. Morcrette, 2011: Global Climate. Aerosols [in" State of the Climate in 2010"], B. Am. Meteorol. Soc., 92(6), S65-S67.

Beyer H.-G., Costanzo C., and Heinemann D., 1996. Modifications of the Heliosat procedure for irradiance estimates from satellite images. Solar Energy, 56, 207-212.

Beyer H. G., Martinez J. P., Suri M., Torres J. L., Lorenz E., Hoyer-Klick C., Ineichen P., 2008. D 1.1.1 Handbook on Benchmarking, Management and Exploitation of Solar Resource Knowledge, CA – Contract No. 038665.

Bird, R., Hulstrom, R., 1981. Review, evaluatoin and improvement of direct irradiance models. Journal of Solar Energy Engineering 103, 182–192.

Blanc P., Wald L., 2012. The SG2 algorithm for a fast and accurate computation of the position of the Sun. Solar Energy, 86, 3072-3083, doi: 10.1016/j.solener.2012.07.018.

Blanc, P., B. Gschwind, M. Lefèvre, L. Wald, 2014a: Twelve monthly maps of ground albedo parameters derived from MODIS data sets. In Proceedings of IGARSS 2014, held 13-18 July 2014, Quebec, Canada, USBKey, pp. 3270-3272.

Blanc, P., B. Espinar, N. Geuder, C. Gueymard, R. Meyer, R. Pitz-Paal, B. Reinhardt, D. Renné, M. Sengupta, L. Wald, S. Wilbert, 2014b. Direct normal irradiance related definitions and applications: The circumsolar issue, Solar Energy, 110, 561-577.

Cano, D., Monget, J., Albuisson, M., Guillard, H., Regas, N., and Wald, L., 1986. A method for the determination of the global solar radiation from meteorological satellite data. Solar Energy, 37, 31-39.

Collins, W.D., P.J. Rasch, B.E. Eaton, B.V.Khattatov, J.-F. Lamarque, 2001. Simulating aerosols using a chemical transport model with assimilation of satellite aerosol retrievals: Methodology for INDOEX, J. Geophys. Res 106, D7, 7313-7336.

Diabaté L., Demarcq H., Michaud-Regas N., Wald L., 1988. Estimating incident solar radiation at the surface from images of the Earth transmitted by geostationary satellites: the Heliosat Project. International Journal of Solar Energy, 5, 261-278.

Diabaté L., Moussu G., Wald L., 1989. Description of an operational tool for determining global solar radiation at ground using geostationary satellite images. Solar Energy, 42(3), 201-207.

Eissa, Y., Munawwar, S., Oumbe, A., Blanc, P., Ghedira, H., Wald, L., Bru, H., and Goffe, D.: Validating surface downwelling solar irradiances estimated by the McClear model under cloud-free skies in the United Arab Emirates, Solar Energy, 114, 17-31, 2015, doi:10.1016/j.solener.2015.01.017.

Espinar B., Ramírez L., Polo J., Zarzalejo L.F., Wald L., 2009. Analysis of the influences of uncertainties in input variables on the outcomes of the Heliosat-2 method. Solar Energy, 83, 1731-1741, doi:10.1016/j.solener.2009.06.010.

Farr T. G. et al. . The Shuttle Radar Topography Mission. Reviews of Geophysics. 45, RG, doi: 10.1029/2005RG000183(2007) (2004).

Geiger, M., Diabate, L., Menard, L., Wald, L., 2002. A web service for controlling the quality of measurements of global solar irradiation. Solar Energy 73, 475–480.

GEOSS, 2005. The Global Earth Observation System of Systems (GEOSS) 10-Year Implementation Plan (As adopted 16 February 2005), http://www.earthobservations.org/documents/10-Year%20Implementation%20Plan.pdf

Gesch, D.B., and Larson, K.S., 1996. Techniques for development of global 1-kilometer digital elevation models. In: Pecora Thirteen, Human Interactions with the Environment - Perspectives from Space, Sioux Falls, South Dakota, August 20-22, 1996.

Greuell, W., R. Roebeling, 2009: Toward a standard procedure for validation of satellite-derived cloud liquid water path: A study with SEVIRI data, J. Appl. Meteorol. Climatol., 48, 1575–1590.

Grüter W., Guillard H., Möser W., Monget J.M., Palz W., Raschke E., Reinhardt R.E., Schwarzmann P., Wald L., 1986. Solar radiation data from satellite images. Solar Energy R&D in the European Communities, series F: Solar Radiation Data, vol. 4, D. Reidel Publishing Co., 100 p.

Gschwind B., Ménard L., Albuisson M., Wald L., 2006. Converting a successful research project into a sustainable service: the case of the SoDa Web service. Environmental Modelling and Software, 21, 1555-1561, doi:10.1016/j.envsoft.2006.05.002.

Gschwind B., Wald L., Mahl R., Irigoin F., Ménard L., 2007. Test of several approaches for the composition of web services in meteorology. In Proceedings of EnviroInfo 2007, Environmental Informatics and systems research, the 21st International Conference on “Informatics for Environmental Protection”, Warsaw, Poland, 2007, vol. 1 “Plenary and session papers”, p. 127-133, ISBN 978-3-8322-6397-3.

Gschwind, B., Wald L., Blanc, P., Lefèvre, M., Schroedter-Homscheidt, M., Arola, A., 2019. Improving the McClear model estimating the downwelling solar radiation at ground level in cloud free conditions – McClear-V3., Meteorol. Z./Contrib. Atm. Sci., 28, 2, 147-163, doi:10.1127/metz/2019/0946.

Hammer, A., Heinemann, D., Westerhellweg, A., 1998. Derivation of Daylight and Solar Irradiance Data from Satellite Observations', Proceeding of the 9th Conference on Satellite Meteorology and Oceanography, Paris, France, 25.05.-29.05.1998, pp747-750,

available at https://uol.de/fileadmin/user_upload/physik/ag/ehf/enmet/publications/solar/conference/1998/Derivation_of_Daylight_and_Solar_Irradiance_Data_from_Satellite_Observations.pdf.

Hess, M., P. Koepke, I. Schult, 1998: Optical properties of aerosols and clouds: The software package OPAC. B. Am. Meteorol. Soc., 79, 831–844.

Hoyer-Klick C., Schillings C., Schroedter Homscheidt M., Beyer H.-G., Dumortier D., Wald L., Menard L., Gschwind B., Martinoli M., Gaboardi E., Ramirez L., Polo J., Huld T., Suri M., Cebecauer T., De Blas M., Lorenz E., Pfatischer R., Remund J., Ineichen P., Tsvetkov A., Hofierka J., 2008. Management and exploitation of solar resource knowledge. Proceedings, EUROSUN 2008, 1st International Congress on Heating, Cooling and Buildings, Lisbon, Portugal (2008).

Hoyer-Klick, C., Schillings, C., Stökler, S., 2016. Satellite based estimation of solar radiation applied at DLR, SolarMedAtlas documentation available at http://www.solar-med-atlas.org/solarmed-atlas/download/DLR%20Heliosat%20Method.pdf.

Ineichen, P., Perez, R., 2002. A new airmass independent formulation for the Linke turbidity coefficient, Solar Energy, 73, 3, 151–157.

Inness, A., Ades, M., Agustí-Panareda, A., Barré, J., Benedictow, A., Blechschmidt, A.-M., Dominguez, J. J., Engelen, R., Eskes, H., Flemming, J., Huijnen, V., Jones, L., Kipling, Z., Massart, S., Parrington, M., Peuch, V.-H., Razinger, M., Remy, S., Schulz, M., and Suttie, M., 2019: The CAMS reanalysis of atmospheric composition, Atmos. Chem. Phys., 19, 3515–3556, https://doi.org/10.5194/acp-19-3515-2019 .

Iqbal, M., 1983. An Introduction to Solar Radiation. Academic Press, New York.

ISO, 1995. Guide to the Expression of Uncertainty in Measurement, first ed. International Organization for Standardization, Geneva, Switzerland.

Kato, S., Ackerman, T. P., Mather, J. H., and Clothiaux, E. , 1999: The k–distribution method and correlated–k approximation for a shortwave radiative transfer model, J. Quant. Spectrosc. Radiat. Transfer, 62, 109–121.

Kinne, S., Schulz, M., Textor, C., Guibert, S., Balkanski, Y., Bauer, S., Bernsten, T., Berglen, T., Boucher, O., Chin, M., Collins, W., Dentener, F., Diehl, T., Easter, R., Feichter, J., Fillmore, D., Ghan, S., Ginoux, P., Gong, S., Grini, A., Hendricks, J., Herzog, M., Horowitz, L., Isaksen, I., Iversen, T., Kikevag, A., Kloster, S., Koch, D., Kristjansson, J., Krol, M., Lauer, A., Lamaraque, J., Lesins, G., Liux, X., Lohmann, U., Montanaro, V., Myhre, G., Penner, J., Pitari, G., Reddy, S., Seland, O., Stier, P., Takemura, T., Tie, X., 2006. An AeroCom initial assessment - optical properties in aerosol component modules of global models. Atmospheric Chemistry and Physics, 6, 1815-1834.

Klüser, L., Killius, N., Gesell, G., 2015: APOLLO_NG – a probabilistic interpretation of the APOLLO legacy for AVHRR heritage channels, Atmos. Meas. Tech., 8, 4155-4170.

Kriebel, K.T., R.W. Saunders and G. Gesell, 1989: Optical Properties of Clouds Derived from Fully Cloudy AVHRR Pixels. Beiträge zur Physik der Atmosphäre, Vol. 62, No. 3, pp. 165-171, August 1989

Kriebel K. T., Gesell G., Kästner M., Mannstein H., 2003: The cloud analysis tool APOLLO: Improvements and Validation, Int. J. Rem. Sens., 24, 2389-2408.

Koepke, P., 1989: Removal of Atmospheric Effects from AVHRR Albedos, Journ. Appl. Met., Vol 28, 1341-1348.

Laguarda, A., Giacosa, G., Alonso-Suarez, R., Abal, G., 2020: Performance of the site-adapted CAMS database and locally adjusted cloud index models for estimating global solar horizontal irradiation over the Pampa Húmeda, Sol. Energy, 199, 295-307, doi:/10.1016/j.solener.2020.02.005.

Lefèvre M., Diabaté L., Wald L., 2007. Using reduced data sets ISCCP-B2 from the Meteosat satellites to assess surface solar irradiance. Solar Energy, 81, 240-253, ddoi:10.1016/j.solener.2006.03.008.

Lefèvre, M., A. Oumbe, P. Blanc, B. Espinar, B. Gschwind, Z. Qu, L. Wald, M. Schroedter-Homscheidt, C. Hoyer-Klick, A. Arola, A. Benedetti, J. W. Kaiser, J.-J. Morcrette, 2013. McClear: a new model estimating downwelling solar radiation at ground level in clear-sky conditions. Atmospheric Measurement Techniques, 6, 2403-2418, doi: 10.5194/amt-6-2403-2013.

Lefèvre, M., and Wald, L., 2016: Validation of the McClear clear-sky model in desert conditions with three stations in Israel. Advances in Science and Research, 13, 21-26, doi:10.5194/asr-13-21-2016.

Marchand, M., Al-Azri, N., Oumbe-Ndeffotsing, A., Wey, E., and Wald, L., 2017: Evaluating meso-scale change in performance of several databases of hourly surface irradiation in South-eastern Arabic Peninsula, Adv Sci Res, 14, 7-15, doi:10.5194/asr-14-7-2017.

Mayer, B., A. Kylling, 2005: Technical note: The libRadtran software package for radiative transfer calculations - description and examples of use, Atmos. Chem. Phys., 5, 1855-1877, doi:10.5194/acp-5-1855-2005.

McPeters, R., Bhartia, P., Krueger, A., Herman, C., Wellmeyer, C., Seftor, C., Jaross, G., Torres, O., Moy, L., Labow, G., Byerly,W.,Taylor, S., Swissler,T., Cebula, R., 1998. Earth probe total ozone mapping spectrometer (toms) dataproducts user's guide.Tech.rep., NASATechnical Publication 1998-206895.

Ménard L., Wald L., Blanc Ph., Ranchin T., 2009. Sitting of a solar power plant: development of Web service based on GEOSS data and guidance. In: Proceedings, 33rd International Symposium on Remote Sensing of Environment, ISRSE 33, Stresa, Italy, May 4-8, 2009, paper 789, [USB key].

Morcrette, J.-J., O. Boucher, L. Jones, D. Salmond, P. Bechtold, A. Beljaars, A. Benedetti, A. Bonet, J. W. Kaiser, M. Razinger, M. Schulz, S. Serrar, A. J. Simmons, M. Sofiev, M. Suttie, A.

M. Tompkins, and A. Untch (2009): Aerosol analysis and forecast in the ECMWF Integrated Forecast System. Part I: Forward modelling, J. Geophys. Res., 114D, D06206, doi:10.1029/2008JD011235.

Möser, W. and Raschke, E., 1984. Incident solar radiation over Europe estimated from Meteosat data. Journal of Applied Meteorology, 23, 166-170.

Mueller, R., Dagestad, K., Ineichen, P., Schroedter, M., Cros, S., Dumortier, D., Kuhlemann, R., Olseth, J., Piernavieja, G., Reise, C., Wald, L., and Heinnemann, D., 2004. Rethinking satellite based solar irradiance modelling - the SOLIS clear sky module. Remote Sensing of Environment, 91, 160-174.

Ohmura, A., Gilgen, H., Hegner, H., Mueller, G., Wild, M., Dutton, E. G., Forgan, B., Froelich, C., Philipona, R., Heimo, A., Koenig-Langlo, G., McArthur, B., Pinker, R., Whitlock, C. H., and Dehne, K. , 1998: Baseline Surface Radiation Network (BSRN/WCRP): New precision radiometry for climate research, B. Am. Meteorol. Soc., 79, 2115–2136, doi:10.1175/15200477(1998)079<2115:BSRNBW>2.0.CO;2.

Oumbe A., 2009. Exploitation des nouvelles capacités d'observation de la terre pour évaluer le rayonnement solaire incident au sol (Assessment of solar surface radiation using new earth observation capabilities). Thèse de Doctorat, MINES ParisTech, Paris, France, 128 pages).

Oumbe, A., Qu, Z., Blanc, P., Bru, H., Lefèvre, M., and Wald, L., 2012: Modeling circumsolar irradiance to adjust beam irradiances from radiative transfer models to measurements, EMS Annual Meeting 2012, 10–14 September 2012, Lodz, Poland.

Oumbe, A., Qu, Z., Blanc, P., Lefèvre, M., Wald, L., and Cros, S., 2014: Decoupling the effects of clear atmosphere and clouds to simplify calculations of the broadband solar irradiance at ground level. Geoscientific Model Development, 7, 1661-1669, doi:10.5194/gmd-7-1661-2014. Corrigendum, 7, 2409-2409, 2014.

Peel, M. C., Finlayson, B. L., McMahon, T. A., 2007: Updated world map of the Köppen-Geiger climate classification. Hydrol. Earth Syst. Sci., 11, 1633-1644.

Perez R., Seals R., Zelenka A., 1997. Comparing satellite remote sensing and ground network measurements for the production of site/time specific irradiance data. Solar Energy, 60, 89–96.

Qu, Z., Gschwind, B., Lefevre, M., and Wald, L., 2014: Improving HelioClim-3 estimates of surface solar irradiance using the McClear clear-sky model and recent advances in atmosphere composition. Atmospheric Measurements Techniques, 7, 3927–3933, doi:10.5194/amt-7-3927-2014.

Qu, Z., Oumbe, A., Blanc, P., Espinar, B., Gesell, G., Gschwind, B., Klüser, L., Lefèvre, M., Saboret, L., Schroedter-Homscheidt, M., and Wald L.., 2017. Fast radiative transfer parameterisation for assessing the surface solar irradiance: The Heliosat-4 method, Meteorologische Zeitschrift, 26, 33-57, doi: 10.1127/metz/2016/0781.

Reinhardt, B., R. Buras, L. Bugliaro, B. Mayer, S. Wilbert, 2012: Circumsolar radiation- a reason for solar resource overestimation – Globally characterized, EMS Annual Meeting 2012, 10-14 September 2012, Lodz, Poland.

Remund J., Wald L., Lefèvre M., Ranchin T., Page J., 2003. Worldwide Linke turbidity information. In Proceedings of ISES Solar World Congress, 16-19 June, Göteborg, Sweden, CD-ROM published by International Solar Energy Society.

Remy, S., Z. Kipling, J. Flemming, O. Boucher, P. Nabat, M. Michou, A. Bozzo, M. Ades, V. Huijnen, A. Benedetti, R. Engelen, V.-H. Peuch, J.-J. Morcrette, 2019: Description and evaluation of the tropospheric aerosol scheme in the Integrated Forecasting System (IFS-AER, cycle 45R1) of ECMWF, Geosci. Model. Dev., 12, 4627-4659, doi:10.5194/gmd-12-4627-2019.

Rigollier C., Bauer O., Wald L., 2000. On the clear sky model of the 4th European Solar Radiation Atlas with respect to the Heliosat method. Solar Energy, 68(1), 33-48.

Rigollier C., Lefèvre M., Wald L., 2004. The method Heliosat-2 for deriving shortwave solar radiation from satellite images. Solar Energy, 77(2), 159-169.

Roebeling, R.A., A.J. Feijt, P. Stammes, 2006: Cloud property retrievals for climate monitoring: Implications of differences between Spinning Enhanced Visible and Infrared Imager (SEVIRI) on METEOSAT-8 and Advanced Very High Resolution Radiometer (AVHRR) on NOAA-17, Journ. Geophys. Res., 111, D20210, doi:10.1029/2005JD006990.

Schade, N. H., A. Macke, H. Sandmann, C. Stick, 2007: Enhanced solar global irradiance during cloudy sky conditions. Meteor. Z., 16, 295–304.

Schaaf, C. B., F. Gao, A. H. Strahler, W. Lucht, X. W. Li, T. Tsang, N. C. Strugnell, X. Y. Zhang, Y. F. Jin, J. P. Muller, P. Lewis, M. Barnsley, P. Hobson, M. Disney, G. Roberts, M. Dunderdale, C. Doll, R. P. d'Entremont, B. X. Hu, S. L. Liang, J. L. Privette, D. Roy, 2002: First operational BRDF, albedo nadir reflectance products from MODIS, Remote Sens. Environ., 83, 135-148, doi:10.1016/S0034-4257(02)00091-3.

Schroedter-Homscheidt, M., Azam, F., Betcke, J., Hanrieder, N., Lefèvre, M., Saboret, L., Saint-Drenan, Y.-M.: Surface solar irradiation retrieval from MSG/SEVIRI based on APOLLO Next Generation and HELIOSAT-4 methods, Contrib. Atm. Sci./Meteorol. Z.,2022, doi:10.1127/metz/2022/1132

Schutgens, N. A. J., R. A. Roebeling, 2009: Validating the validation: the influence of liquid water distribution in clouds on the intercomparison of satellite and surface observations, J. Atmos. Oceanic Technol., 26, 1457–74, doi: 10.1175/2009jtecha1226.1.

Shiobara, M., S. Asano, 1993: Estimation of cirrus optical thickness from sun photometer measurements, J. Appl. Meteor., 33, 672-681, doi: 10.1175/1520-0450(1994)033<0672:EOCOTF>2.0.CO;2.

Stephens, G.L., S. Ackerman, E. A. Smith, 1984: A Shortwave Parameterization Revised to Improve Cloud Absorption, Journ. Atm. Scienc., Vol 41, no 4, 687-690.

Tarpley, J., 1979. Estimating incident solar radiation at the surface from geostationary satellite data. Journal of Applied Meteorology, 18, 1172-1181.

Taylor, V.R., L.L. Stowe, 1983: Atlas of Reflectance Patterns for Uniform Earth and Cloud surfaces (NIMBUS-7 ERB--61 Days), NOAA Technical Report NESDIS 10.

Tegen, I., Hollring, P., Chin, I., Fung, D., D., J., Penner, J., 1997. Contribution of different aerosol species to the global aerosol extinction optical thickness: Estimates from model results. Journal of Geophysical Research 102, 23895–23915.

Thomas, C., Wey, E., Blanc, P., Wald, L., and Lefèvre, M., 2016a: Validation of HelioClim-3 version 4, HelioClim-3 version 5 and MACC-RAD using 14 BSRN stations, Energy Procedia, 91, 1059-1069, doi: 10.1016/j.egypro.2016.06.275.

Thomas, C., Wey, E., Blanc, P., and Wald, L., 2016b: Validation of three satellite-derived databases of surface solar radiation using measurements performed at 42 stations in Brazil, Adv Sci Res, 13, 81-86, doi:10.5194/asr-13-81-2016.

Vermote, E.F., D. Tanré, J. L. Deuzé, M. Herman, J.-J. Morcrette, 1997: Second simulation of the satellite signal in the solar spectrum: An overview, IEEE T. Geosci. Remote Sens., 35, 675–686.

Wahab, A. M., El Metwally M., Hassan R., Lefèvre M., Oumbe A., Wald L., 2009. Assessing surface solar irradiance in Northern Africa desert climate and its long-term variations from Meteosat images. International Journal of Remote Sensing, 31(01), 261-280.

Wald L., Albuisson M., Best C., Delamare C., Dumortier D., Gaboardi E., Hammer A., Heinemann D., Kift R., Kunz S., Lefèvre M., Leroy S., Martinoli M., Ménard L., Page J., Prager T., Ratto C., Reise C., Remund J., Rimoczi-Paal A., Van der Goot E., Vanroy F., and Webb A., 2002. SoDa: a project for the integration and exploitation of networked solar radiation databases. In: Environmental Communication in the Information Society, W. Pillmann, K. Tochtermann Eds, Part 2, pp. 713-720. Published by the International Society for Environmental Protection, Vienna, Austria.

Wald L., Albuisson M., Best C., Delamare C., Dumortier D., Gaboardi E., Hammer A., Heinemann D., Kift R., Kunz S., Lefèvre M., Leroy S., Martinoli M., Ménard L., Page J., Prager T., Ratto C., Reise C., Remund J., Rimoczi-Paal A., Van der Goot E., Vanroy F., and Webb A., 2004. SoDa: a Web service on solar radiation. In Proceedings of Eurosun 2004, published by PSE GmbH, Freiburg, Germany, pp. (3)921-927, ISBN 3-9809656-4-3.

WMO, 1981. Technical Note N° 172, WMO-No. 554, World Meteorological Organization, Geneva, Switzerland, pp. 121-123.

WMO: Guide to meteorological instruments and methods of observation, WMO-No 8, 2008 edition updated in 2010, World Meteorological Organization, Geneva, Switzerland, 2012.

Zelenka A., Perez R., Seals R., Renne´ D., 1999. Effective accuracy of satellite-derived hourly irradiances. Theoretical and Applied Climatology, 62, 199–207.

Zender, C. S., H. Bian, and D. Newman, 2003. Mineral Dust Entrainment And Deposition (DEAD) model: Description and 1990s dust climatology. J. Geophys. Res., 108(D14), 4416, doi:10.1029/2002JD002775.

Copernicus Atmosphere Monitoring Service

ECMWF - Shinfield Park, Reading RG2 9AX, UK

Contact: info@copernicus-atmosphere.eu